Understanding disease suppressive soils: molecular and chemical identification of microorganisms and mechanisms involved in soil suppressiveness to Fusarium culmorum of wheat

Ossowicki, A.S.

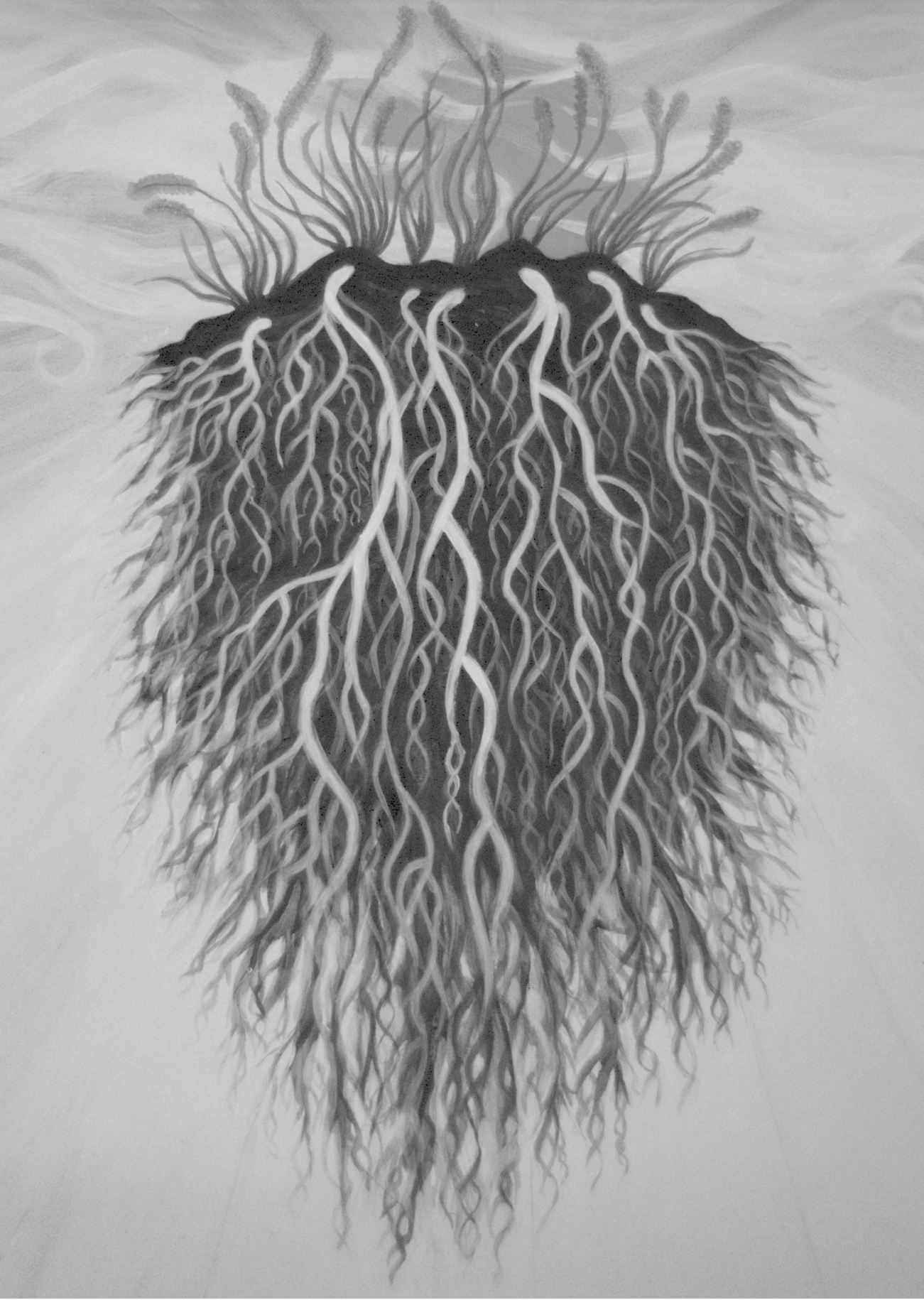

Chapter 2

Microbial and volatile profiling of soils suppressive to *Fusarium culmorum* of wheat

Adam Ossowicki[1*], Vittorio Tracanna[2*], Marloes L. C. Petrus[3], Gilles van Wezel[3], Jos M. Raaijmakers[1,3], Marnix H. Medema[2#] and Paolina Garbeva[1#]

1. Department of Microbial Ecology, Netherlands Institute of Ecology (NIOO-KNAW), Wageningen, The Netherlands
2. Bioinformatics Group, Wageningen University, Wageningen, The Netherlands
3. Institute of Biology, University of Leiden, Leiden, The Netherlands

Published in Proceedings of the Royal Society B
https://doi.org/10.1098/rspb.2019.2527

Abstract

In disease-suppressive soils, microbiota protect plants from root infections. Bacterial members of this microbiota have been shown to produce specific molecules that mediate this phenotype. To date, however, studies have focused on individual suppressive soils and the degree of natural variability of soil suppressiveness remains unclear. Here, we screened a large collection of field soils for suppressiveness to *F. culmorum* using wheat (*Triticum aestivum*) as a model host plant. A high variation of disease suppressiveness was observed, with 14% showing a clear suppressive phenotype. The microbiological basis of suppressiveness to *F. culmorum* was confirmed by gamma-sterilization and soil transplantation. Amplicon sequencing revealed diverse bacterial taxonomic compositions and no specific taxa were found exclusively enriched in all suppressive soils. Nonetheless, co-occurrence network analysis revealed that two suppressive soils shared an overrepresented bacterial guild dominated by various *Acidobacteria*. In addition, our study revealed that volatile emission may contribute to suppression, but not for all suppressive soils. Our study raises new questions regarding the possible mechanistic variability of disease suppressive phenotypes across physicochemically different soils. Accordingly, we anticipate that larger-scale soil profiling, along with functional studies, will enable a deeper understanding of disease suppressive microbiomes.

Introduction

The phenomenon of soil disease suppressiveness has been recognized for almost a century and was first defined by Cook and Baker (Cook and Baker, 1983) as soils where a particular soil-borne disease does not develop, despite the presence of the virulent pathogen, a susceptible host and favorable conditions for disease development. Physical and chemical properties of the soil can play a role in this phenomenon, but in many cases disease suppressiveness is microbial in nature (Andrade et al., 2011; Cha et al., 2016; Weller et al., 2002b; Wiseman et al., 1996).

Two types of soil suppressiveness can be distinguished, namely general and specific. General suppression is effective against a range of pathogens, whereas specific suppression operates against only one or a few of them. General soil suppressiveness is a result of the activity of the overall soil microbial community, whereas specific soil suppressiveness is due to the concerted action of specific microbial genera that interfere at some stage of the life cycle of the soil-borne pathogen. Specific soil suppressiveness can be eliminated by selective heat treatments and is transferable to a conducive soil by mixing in a small amount (1-10%) of suppressive soil (for review: (Mazzola, 2002; Schlatter et al., 2017a)).

For many suppressive soils the microorganisms and mechanisms have not been elucidated. Some of the best-studied suppressive soils to date are the take-all-decline (TAD) soils, where

root disease of wheat or barley caused by the fungal pathogen *Gaeumanomyces graminis* var. *tritici* is suppressed (Cook and Rovira, 1976; Duran et al., 2017; Hornby, 1983). Suppressiveness to take-all disease is, at least in part, due to the enrichment of populations of root-associated *Pseudomonas* spp. producing the antifungal polyketide 2,4-diacetylphloroglucinol (2,4-DAPG) (Kwak et al., 2011; Raaijmakers et al., 1999; Raaijmakers and Weller, 1998; Weller et al., 2002b). For Fusarium-wilt-suppressive soils, the microbes and mechanisms identified so far involve non-pathogenic *Fusarium oxysporum* and *Pseudomonas* species that, in a complementary manner, compete with pathogenic *F. oxysporum* for carbon and iron(Alabouvette, 1986; Duijff et al., 1999; Siegel-Hertz et al., 2018b). Recent studies on soils suppressive to *Rhizoctonia* damping-off disease of sugar beet revealed the involvement of multiple bacterial genera belonging to the Pseudomonadaceae, Streptomycetaceae and Burkholderiacea*e*. The suppression was linked to the production of antifungal lipopeptide thanamycin by *Pseudomonas* and to the production of volatile metabolites by *Streptomyces* spp*.* and *Paraburkholderia graminis* (Carrion et al., 2018; Viviane Cordovez et al., 2015; Duran et al., 2017). Volatiles are low-molecular-mass metabolites involved in long-distance interactions with potent antimicrobial activities (Cho et al., 2017; Garbeva et al., 2014a, 2011; Ossowicki et al., 2017). For example, the effects of volatiles emitted from 50 agricultural soils on two soil-borne pathogenic fungi (*F. oxysporum, R. solani*) and a plant pathogenic oomycete (*Pythium intermedium*) have recently been studied (van Agtmaal et al., 2018). This work showed that most soils emit volatiles that inhibit hyphal growth, but the extent of growth inhibition per soil differed strongly for the three pathogens.

To date, most studies on suppressive soils have been limited to a single field soil. Except for the case of the TAD soils (Landa et al., 2002), it is currently unclear how widespread suppressiveness to specific pathogens is as a biological phenomenon. Furthermore, it is not established yet whether suppression is mediated by one or multiple taxa and mechanisms across various suppressive soils. Finally, the role of volatiles in soil suppressiveness in the presence of both the pathogen and the host plant is yet unexplored.

In this study, we screened a large collection of field soils for suppressiveness to *Fusarium culmorum*, a ubiquitous soil-borne fungus causing foot rot, root rot and Fusarium head blight of different cereals, in particular wheat and barley (Wiese, 1987). Using wheat (*Triticum aestivum*) as the host plant, we found *F. culmorum* suppressiveness in 4 out of 28 soils.

We hypothesised that 1) soils suppressive to *F. culmorum* have similar rhizobacterial community compositions with specific enriched taxa, 2) volatile compounds contribute to disease suppression against *F. culmorum,* and 3) disease-suppressive soils have similar volatile profiles. We anticipated that specific rhizobacterial taxa and volatiles correlate with

soil suppressiveness against *F. culmorum*. However, our comparative analysis of bacterial rhizosphere microbiome composition of suppressive and non-suppressive (conducive) soils, along with volatile profiling, indicates that the phenomenon may be mediated by different rhizobacterial genera across these soils and that volatiles may contribute to the suppressive phenotype only for a limited number of soils.

Materials and Methods

Soil collection

In order to examine soil disease suppressiveness to *F. culmorum*, 28 sites in the Netherlands and Germany were chosen based on information on soil type and crop rotation. The sites included 25 arable fields, 2 pastures and 1 forest. The arable fields included sites with wheat present in crop rotation over the last three years and sites without wheat present in the available history of the field.

Soil samples were collected in the period from January to April 2017 from 3-meter squares located in the middle of each agricultural field/pasture. In this area, top soil cores of approximately 30 cm deep were extracted. Samples were air-dried in room temperature, homogenized, sieved through 4 mm sieve and stored at 4°C. Heavy clay-type soils were additionally flaked using a jaw-crusher (Type BB-1, Retsch, Germany) after drying. Soil physical and chemical parameters were measured as described in Supplementary material part I.

Wheat growth conditions and pathogen inoculation

All the greenhouse experiments were performed in growth cabinets (MC 1750 VHO-EVD, Snijders Labs) in 20°C day and night, photoperiod 12h day /12h night and 60 % relative humidity. In all the experiments, surface-sterilized and pre-germinated wheat seeds (JB Asano from Agrifirm, Netherlands) were used. Plants were watered every second day and weekly supplemented with 0.5 Hoagland solution (1ml per 80 cc of the soil, 0.5M $Ca(NO_3)_2{\cdot}4H_2O$, 1M KNO_3, 1M KH_2PO_4, 0.5M $MgSO_4{\cdot}7H_2O$ and 98.6 mM ferric EDTA).

As a standard substrate, we used a dune soil collected near Bergharen, the Netherlands (BS) (Schulz-Bohm et al., 2015). Before use, BS was air-dried, sieved and gamma-sterilized (Synergy Health Ede B.V., the Netherlands). Sub-samples of eight soils from the collection were gamma-sterilized as well in the same conditions for later use.

Prior to screening for disease suppressiveness, all soils were “activated” in order to induce microbial activity in a so-called microbiome activation step. For this, soils hosted the growth of wheat for two weeks in the conditions indicated above. After this, plants, including their whole root system, were removed and the remaining soil with activated microbiome was mixed properly.

The soil-borne pathogen *Fusarium culmorum* PV (Blom et al., 2011) was grown on 1/2 PDA media (Oxoid, the Netherlands) and maintained in continuous culture. For plant inoculation, the fungus was transferred to 1/4 PDA and grown for 2 weeks in 20°C. After the incubation, 6mm plugs were cut from the border zone of *Fusarium* hyphae and mixed with the growth substrate (1 plug per 10 cc). Controls without pathogen were inoculated with sterile 1/4 PDA plugs. At the end of the experiments disease symptoms were assessed and plants were used for rhizosphere DNA extraction and sequencing analysis (see Supplementary material part I).

Disease suppressiveness screening

Initial disease suppressiveness screening was performed in propagation trays containing 140 single pots (Teku, the Netherlands) each containing 38cc of soil per pot. In order to minimize the physicochemical differences between the 28 soils, after the activation step (described in paragraph above) the natural soil was mixed 2:1:1 in volume with sterile BS soil and sterile vermiculite (Agra-vermiculite, the Netherlands). The soil was inoculated with *Fusarium* or mock-inoculated with agar plugs, and one seedling was placed in the center of each pot. Plants were grown in ten replicates per treatment and, after three weeks, disease symptoms were assessed (see Supplementary material part I). As a control, we used BS mixed with vermiculite 3:1 in volume.

Confirmation of disease suppressiveness with soils sterilization

Four suppressive and four conducive soils were selected to confirm the previously observed levels of suppressiveness. The confirmation test was performed identically as the screening test but the system was scaled up to 380 cc soil per pot (7x7x8 cm, Teku, the Netherlands) with three plants in each. An additional treatment was included - sterilized soil inoculated with pathogen. Sterile BS, vermiculite mix was used as a control. All the treatments had an additional control without pathogen.

Transplantation assay

To assess whether soil suppressiveness is transferable, we mixed natural soils in proportions 1:9 and 3:7 in volume with a conducive substrate consisting of sterile BS and vermiculite. This experiment was also performed with 380 cc soil per pot (7x7x8 cm), each containing three plants, in treatments with and without the addition of the pathogen. Sterile BS and vermiculite mixture was used as a control.

Sequencing and bioinformatics analysis

Rhizosphere DNA extraction, sequencing, 16S rRNA amplicon data processing and analysis are described in Supplementary material part I.

Effects of soil-emitted volatiles on fungal growth

Assays were performed as previously described by Garbeva et al. (Garbeva et al., 2014a) with small modifications, see Supplementary material part I.

Effects of soil-emitted volatile compounds on disease suppression

The eight soils selected in the suppressiveness screening were tested for their ability to induce soil suppressiveness via volatiles. For this, the modified method described by (Park et al., 2015) was used. Briefly, wheat plants growing in conducive soil mixed with *F. culmorum* plugs were exposed to volatiles emitted by soil present in the compartment below the pot. To avoid any physical contact, compartments were separated and sealed with sterile nylon mesh (Sefar, Switzerland) and paper medical tape as described above. The scheme of the system is shown on figure 3B. Four pots per treatment with three plants per pot were grown for three weeks; afterwards, disease symptoms were assessed.

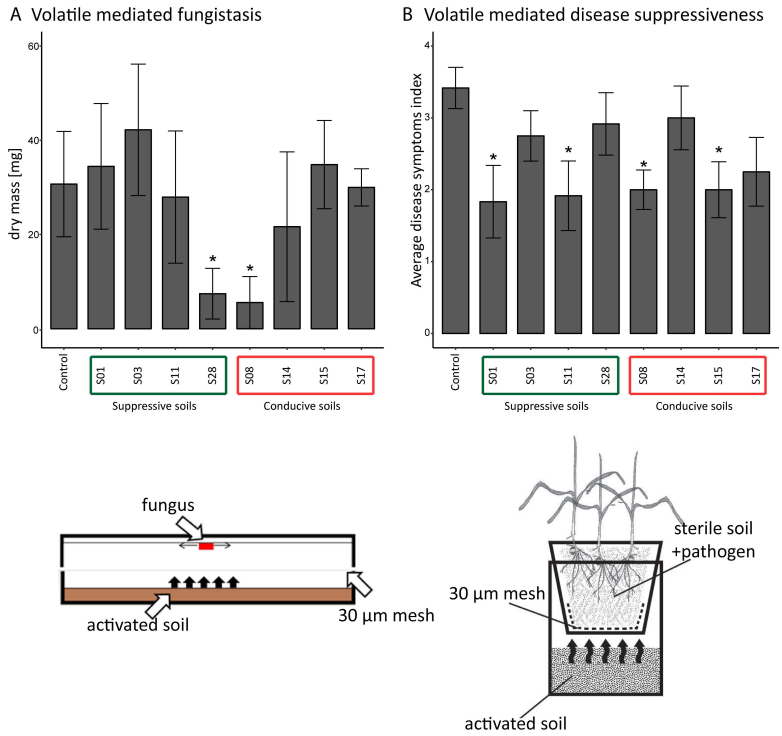

Figure 1. The effect of the volatiles emitted by eight prioritized soils on Fusarium culmorum growth (fungistasis) and disease suppression. (A) Average dry mass of the fungus with standard deviation, the statistically significant differences between treatments and control (based on ANOVA and Tuckey post-hoc test p<0.05) are indicated

by asterisk. (B) Average symptoms index with standard error. The statistically significant differences between treatments and control (based on chi-square test p<0.05) are indicated by asterisk.

Volatile trapping and GC-MS analysis

Volatile compounds were trapped using steel trap containing 150 mg Tenax TA and 150 mg Carbopack B (Markes International Ltd, Llantrisant, UK) and measured using GC-QTOF system. Statistical data analysis was performed using MetaboAnalyst 4.0 software (http://www.metaboanalyst.ca/MetaboAnalyst (Chong et al., 2018)). For details of Volatile trapping and GC-MS analysis, see Supplementary material part I.

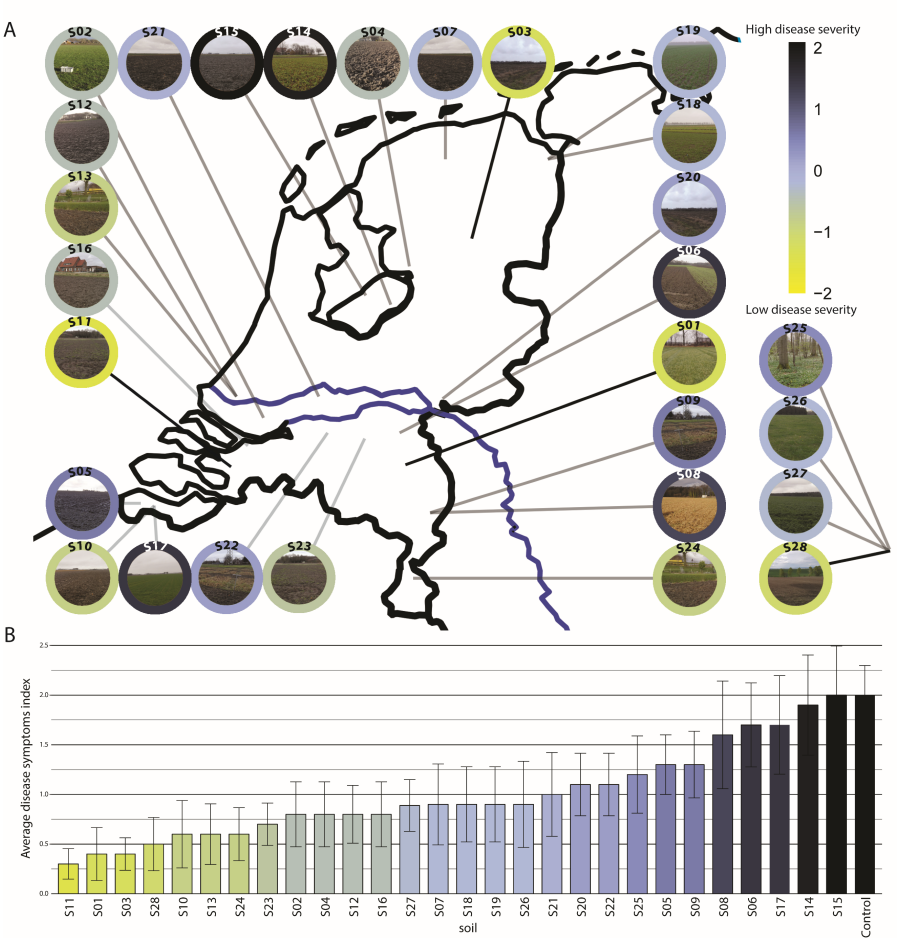

Figure 2. Results of the phenotypic screening towards soil suppressiveness to F. culmorum in 28 soils. (A) Map showing locations of 28 sampling sites and the results of the screening. The color of the outer circle around the photos represents the z-score

transformed average disease symptoms value. Low disease severity indicates soil suppressiveness (yellow color). (B) Bar graph showing average disease symptoms indexes with standard errors.

Results

Identification of soils suppressive to *F. culmorum*

A collection of 28 soils of diverse geographical origins (figure 1A), soil types and agricultural histories (table S1) was screened for disease suppressiveness against *F. culmorum* in greenhouse pot experiments. The disease symptoms of the plants grown in each of the soils were examined three weeks after pathogen inoculation. Overall, high variation in disease suppressiveness was observed between the 28 soils, while being largely consistent between replicates. The disease symptoms across the collection varied from mild or no infection to severe disease. Four soils (S01, S03, S11 and S28 - yellow color, figure 1) showed the lowest level of disease severity with an average score below 0.5 and were considered suppressive (figure 1). Four soils revealed high disease severity with average disease symptoms above 1.5 (S08, S14, S15 and S17 – black color, figure 1) and were considered conducive.

Disease suppression is independent of soil physicochemical properties

In order to investigate phenotypic variation across multiple soil types, our collection included soils from 25 arable fields, 2 pastures and 1 forest, representing different soil types, ranging from sands to heavy clays, with diverse pH (5.3 to 7.8) and C/N ratio (8.8 to 17.5). All physicochemical parameters and field history are summarized in Table S1. No clear correlations between the level of disease suppressiveness and physicochemical parameters and field history were found. Based on canonical correspondence analysis of the 28 soils, there was no separation between disease-suppressive and conducive soils (figure S1, yellow and black dots accordingly). Only weak Pearson correlations were found between physicochemical parameters and disease severity (figure S2). Also, no relevant correlations were found between disease severity and soil pH and C/N ratio (0.24 and 0.25 respectively).

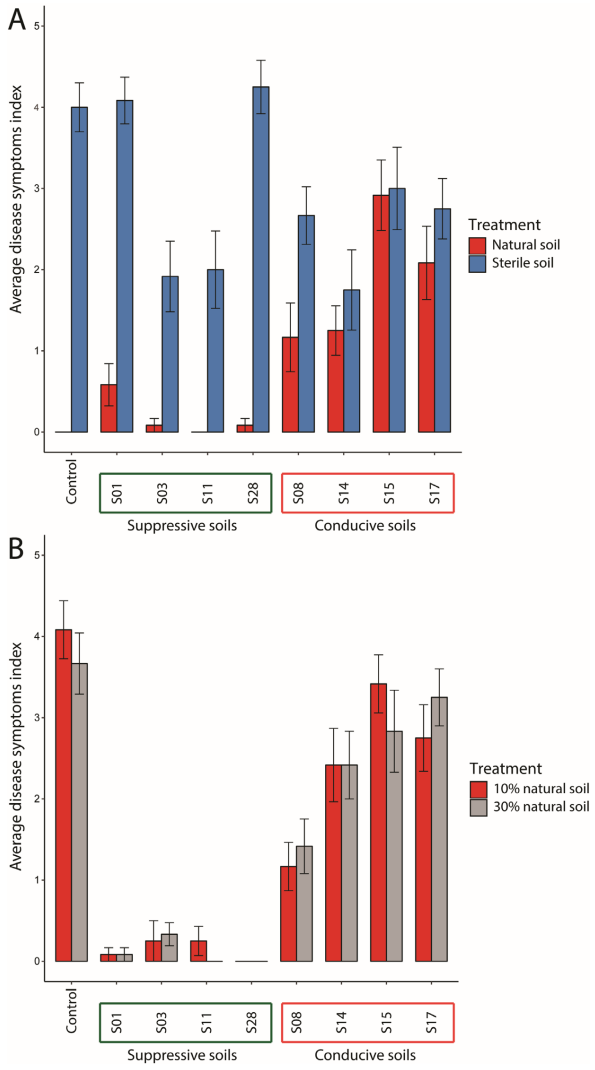

Figure 3. Disease symptoms observed in wheat inoculated with Fusarium culmorum grown in eight prioritized soils. (A) Natural and gamma-sterilized soil with sterile BS soil/vermiculite mix as a control (B) 10% and 30% in volume of natural soil mixed with standardized sterile substrate or with sterile BS soil as a control. The bar indicates the average of the disease symptoms index, with the error bars representing the standard error.

Disease suppressiveness has a microbial basis

Based on the results from the initial screening, a set of eight soils was selected for confirmation assays and further analysis. This included the four soils with the highest level of disease suppressiveness (S01, S03, S11 and S28) and the four conducive soils showing the most contrasting phenotypes (S08, S14, S15 and S17). For the four suppressive soils, low average disease indices were again observed (figure 2A, red bars) but after gamma sterilization, disease indices increased significantly (figure 2A, blue bars). For the four conducive soils, except for S08, gamma sterilization did not substantially enhance disease severity. Furthermore, the results revealed that suppressiveness to *F. culmorum* is

transferable (figure 2B). Mixing 10% or 30% of the suppressive soil (S01, S03, S11 and S28) in a conducive background soil transferred suppressiveness. There was no significant difference in the level of suppression between the transfer of 10% and 30% suppressive soil. Collectively, our data suggest that the microbial community contributes to the suppressive phenotype.

Volatile-mediated inhibition of fungal growth and disease suppression is observed for suppressive and conducive soils

To determine the role of volatile compounds in disease suppression and antifungal activity, the eight selected soils were tested in two experimental systems: i) hyphal growth of *Fusarium* on artificial media exposed to soil volatiles, and ii) plants growing in conducive soil inoculated with the pathogen exposed to soil volatiles (figure 4 A, B and Supplementary material part I). The first assay revealed that only two soils (S28 suppressive and S08 conducive) emitted volatiles that significantly reduced growth of the fungus compared to the control. When plants were exposed to soil volatiles, disease suppression was observed for four out of eight soils (figure 4 B). Again, these included both suppressive (S01, S11) and conducive (S08, S15) soils. Subsequent analysis of volatile profiles emitted by these eight soils did not reveal clear separation between suppressive and conducive soils (figure S3). Interestingly, several suppressive and conducive soils (S03, S08, S11 and S14) revealed very similar volatile profiles. These results suggest that volatiles are not a common mechanism of soil suppressiveness to *F. culmorum*.

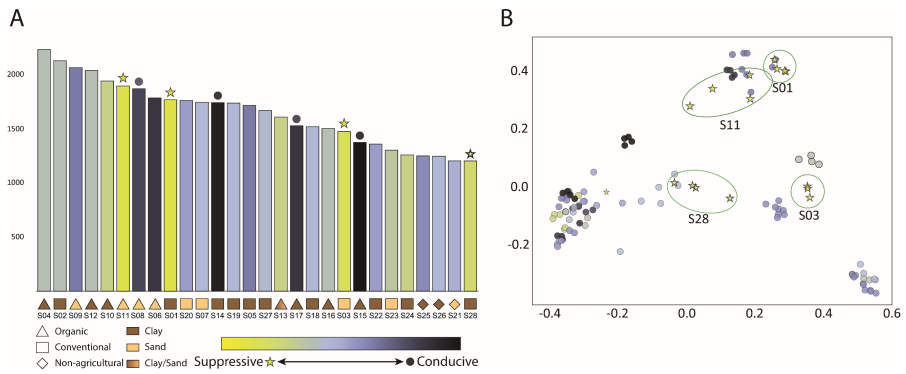

Figure 4. Characteristics of rhizosphere bacterial communities across all 28 soils. (A) Bar plot representing the alpha diversity using the rarefied unique ASV counts. Samples are sorted according to their alpha diversity score and color-coded according to suppressive phenotype. (B) PCoA based on Unweighted UniFrac distance between samples. Circles highlight the suppressive sample replicates clustered together.

Microbial profiling of *F. culmorum*-suppressive soils

To investigate possible links between the rhizobacterial community composition and the disease suppressive phenotype, extensive 16S sequencing was performed for all 28 soils (see Supplementary material part I). The rhizobacterial communities showed large variation between samples and even between replicates of the same samples, as can be seen from the inter- and intra-sample Jaccard similarity of 0.056 (sd = 0.033) and 0.346 (sd = 0.057) respectively. Based on the alpha- and beta-diversity, there were no significant community differences between suppressive and conducive soils. Beta-diversity for all sample pairs was calculated with unweighted UniFrac, which shows consistent grouping for soil sample replicates (figure 4B). Subsequent PCoA analysis of the rhizobacterial community composition of the suppressive and conducive soils indicated that the different suppressive soils have diverse taxonomic compositions and did not group together (figure 4B). This was also the case when calculating community diversity of the samples within specific taxonomic groups (Supplementary figures S4). As for alpha diversity, Wilcoxon rank-sum test showed no significant association between observed ASVs ($p=0.74$) or Shannon diversity ($p=0.07$) and soil suppressiveness. The suppressive soils included both the most and the least diverse communities. The soils from organic farms were associated with higher bacterial diversity compared to the soils from conventional farms and to the non-agricultural soils (figure 4A). Again, there was no consistent correlation between soil suppressiveness and alfa- or beta-diversity.

To establish whether the disease-suppressive phenotypes were mediated by specific rhizobacterial taxon or by multiple taxa, 16S amplicon data were analyzed in more depth. To reveal if one or more individual abundant amplicon sequence variants (ASVs) could be associated with disease suppressiveness, we inspected the presence-absence patterns of all ASVs that were significantly enriched in suppressive soils (figure 5). No individual ASV appeared to be exclusively present in all suppressive samples compared to the conducive samples (figure S5). Random forest classifiers trained on their taxonomic profiles could not predict the suppressive soil phenotype in a leave-one-out analysis. The results were not significantly different when the same analysis was performed using OTU-level clustering of ASVs (at 97% identity).

Co-occurrence network analysis indicates bacterial communities enriched in rhizosphere microbiomes of suppressive soils

To investigate whether specific combinations of ASVs are associated with disease suppressiveness (in subsets of the four suppressive soils), we calculated Spearman correlations between ASV occurrences across all 28 soils and constructed a co-occurrence network from the most highly correlating ASVs in the correlation matrix (see Supplementary material part I). The resulting network (figure 6A) consists of 928 nodes (comprising 21% of

all 4,322 ASVs), distributed across 37 subnetworks. The ASVs in the network that were significantly enriched in suppressive soils are indicated by squares with black border in figure 6B. The subnetworks are taxonomically diverse, with no network being taxonomically homogeneous, even at the phylum level. Interestingly, one of the connected components was found to be particularly associated with the suppressive phenotype. Within this connected component, 7 out of the 163 ASVs were strongly enriched in suppressive soils and these were part of a more densely connected subcomponent comprising 60 ASVs that comprised 6 out of the 7 abovementioned ones. Taxonomic assignments of the suppression-associated subnetwork displayed an overrepresentation of ASVs belonging to different Acidobacteria, namely Blastocatellales and members of subgroup 6, compared to the overall community composition ($p=0.0003$, Fisher exact test, figure 6b). Moreover, several of these Acidobacteria displayed characteristics of being hub taxa in these subnetworks based on their high betweenness centrality. In addition, 11 of the 60 ASVs in the suppressive-associated network were exclusively present in two suppressive soils (figure 6C), 7 of which were taxonomically assigned to Acidobacteria.

Discussion

F. culmorum is an economically important fungal plant pathogen that causes disease in many cereal and non-cereal crops. However, little is known about the occurrence and distribution of soil suppressiveness to this pathogen. To our knowledge, this study is the first to screen for disease suppressiveness in a large collection of diverse soils. Although a high variation in the level of disease suppressiveness was observed between the soils, 14% of the tested soils revealed a clear suppressive phenotype. Interestingly, no physicochemical parameter such as soil type, field history, pH, C/N ratio or content and concentration of bioavailable Fe, K, Mg, P, S correlated with the observed suppressive phenotype. In previous work, physicochemical soil parameters such as soil type, moisture, pH, organic matter and microelements content have been more commonly associated with general disease suppressiveness (Hoper and Alabouvette, 1996; Janvier et al., 2007).

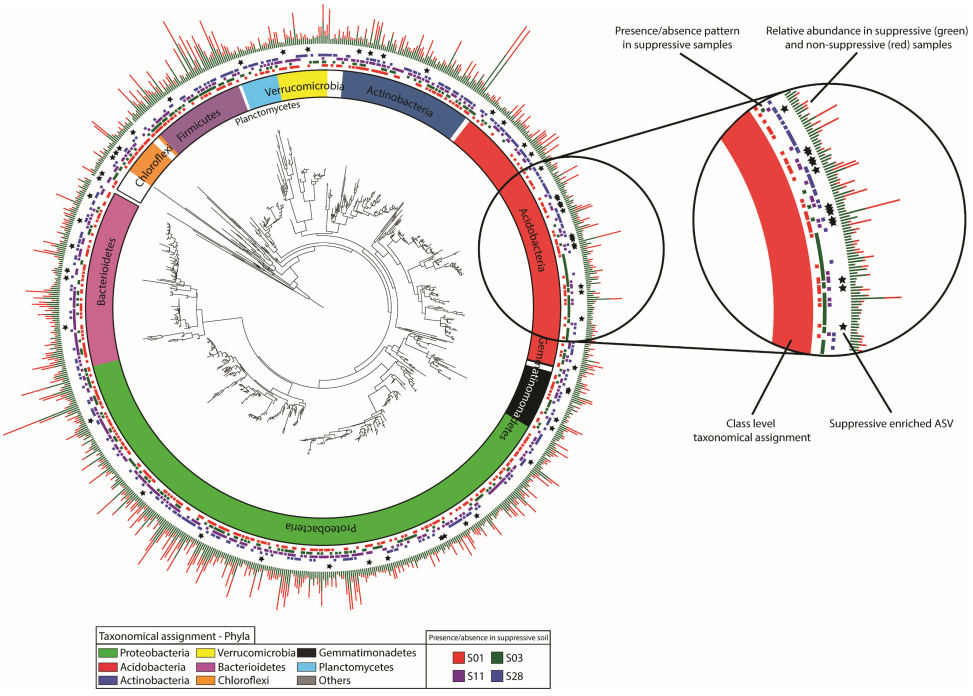

Figure 5. Phylogenetic tree of all ASVs consistently detected in one or more suppressive rhizosphere samples. The rings, from the inside to the outside, represent 1) the taxonomical assignment of the ASVs at the phylum level, 2) the presence/absence patterns of ASVs in the four different suppressive soils, 3) indications (with starts) of ASVs strongly enriched in suppressive samples, and 4) the average cumulative normalized abundance of each ASV in suppressive (green) versus non-suppressive (red) samples. The results show that all ASVs enriched in suppressive samples are specific to a subset of the suppressive soils, while none of the ASVs that occur throughout all suppressive soils are significantly enriched in suppressive versus non-suppressive soils.

In our study, the microbiological basis of specific suppressiveness to *F. culmorum* was revealed by two independent approaches: gamma-sterilization and soil transplantation eliminated and conferred suppressiveness, respectively, and confirmed that suppressiveness to *F. culmorum* was not linked to soil physicochemical parameters but rather to the soil (micro)biome.

Along with the soil, the plant itself is an important determinant of the structure of soil microbial communities and disease suppressiveness. Hence, the strength of disease suppressiveness is attributed to all players in the tripartite relationship of plant-soil-microorganisms (Garbeva et al., 2004). Considering this, in the present study, all

experiments included a “microbiome activation step” by growing wheat for 2 weeks prior screening for disease suppressiveness. The application of plants provides substrates for growth via root exudates and space for the soil microbial community. Several studies have associated disease-suppressive phenotypes to individual bacterial groups based on their relative enrichment compared to a conducive phenotype (Donn et al., 2014; Schlatter et al., 2017a; Yin et al., 2013). However, rhizosphere microbiomes are highly diverse (Charlop-Powers et al., 2015) and multiple differences may exist even between physicochemical similar soils. In the present study, 28 different soils were examined and no individual bacterial taxon was found to be exclusively present or enriched in all suppressive soils. Bacterial taxonomic groups that were more prevalent in some of the suppressive soils were not prevalent in other suppressive soils.

Many studies have aimed to understand the relationship between microbial diversity and disease suppressiveness. However, both low (Mehrabi et al., 2016) and high (Garbeva et al., 2004) community diversity have been associated with soil suppressiveness. Here, we found suppressive samples with both high and low community richness, which suggests community diversity is not the key driver of soil suppressiveness to *Fusarium culmorum*. Community evenness is correlated with the phenotype but the strength of this association is not strong enough ($p=0.07$) to warrant speculations on its role in disease suppressiveness. To our surprise, no ASVs or OTU-level ASV clusters were found to be shared uniquely between the microbial communities of all four suppressive soils, or to be differentially abundant across all these four soils. The fact that random forest classifiers were unable to accurately predict suppressive phenotypes in a leave-one-out analysis of the soils suggests that i) the suppressive phenotypes are mediated by different taxonomic groups across the different suppressive soils and/or ii) that rhizobacteria do not play a major role in suppressiveness to *F. culmorum*. Many functional elements that are known to be able to drive disease suppression (such as biosynthetic gene clusters for secondary metabolites) are often strain-specific and are frequently transferred horizontally across species (Medema et al., 2014). Hence, it is still possible that the same or similar functional elements could drive the suppressiveness across all four soils, while being undetectable by 16S sequencing due to its limited resolution or due to the elements being encoded in the genomes of diverse bacterial taxa.

Representatives of a range of bacterial groups can carry out functions that result in the suppression of soil-borne diseases. For example, several *Bacillus*, *Pseudomonas*, *Streptomyces* or *Flavobacterium* species are well known to play role in suppression of various soil-borne plant pathogens (Cha et al., 2016; Chapelle et al., 2016; Donn et al., 2014; Garbeva et al., 2006; Kwak et al., 2018). However, various previous studies indicate that many of these bacteria reveal antimicrobial activities only as results of interspecific interaction networks (Garbeva et al., 2011; Traxler et al., 2013; Tyc et al., 2017, 2014). The

correlation-based network analysis performed here revealed complex inter-sample connections between individual bacterial taxa that are likely interacting either directly or indirectly, based on their observed co-occurrence. One of the network components provided insights into a bacterial guild that is potentially associated with disease suppressiveness to *Fusarium culmorum*. Multiple ASVs were found to be exclusively present in two distinct disease suppressive microbiomes, while additionally being strongly correlated with another sub-community of ASVs that also consistently occurred in a conducive microbiome. Interestingly, most of these ASVs belonged to *Acidobacteria*. We observe an over-representation of *Acidobacteria* in the suppression associated network when compared to the general community composition (Fisher exact test, p=0.0003). This phylum has previously been associated with *Rhizoctonia solani* bare patch (Yin et al., 2013) and has been shown to harbor diverse species with a large specialized metabolic potential that could be involved in interactions with fungi (Crits-Christoph et al., 2018). Based on their specific enrichment, the identified bacterial guild might represent the suppressive core at the base of the phenotype for two of the four suppressive samples (soils S01 and S11). Further shotgun sequencing efforts as well as microbiological and biochemical analysis are needed to clarify the functional roles of these organisms. Furthermore, one should bear in mind that in addition to the bacterial community structure, the expression of functional genes conferring suppressiveness to soil-borne pathogens might be dependent on interactions with other soil microorganisms such as fungi, protists and viruses.

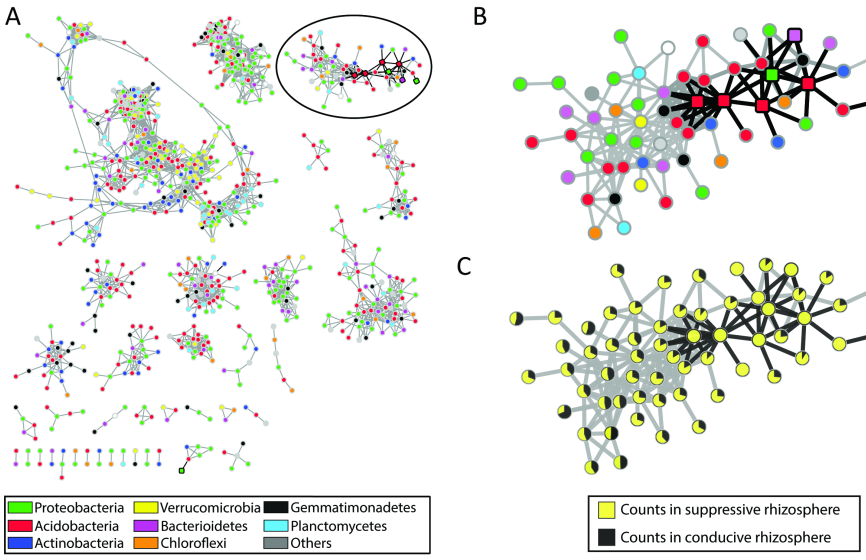

Figure 6. Co-occurrence network analysis of rhizosphere bacteria across samples. A) Complete network of correlated ASVs using Spearman correlation. Nodes represent

individual ASVs; edges link ASVs which had a correlation score above a given threshold. The node color indicates the taxonomical annotation at the phylum level. Edges of ASVs that are significantly enriched in suppressive samples are highlighted black as the respective nodes. B) Zoomed in view of a subnetwork of interest, which shows a number of ASVs associated with the suppressive phenotype indicated by squares with black border, along with its taxonomical distribution. C) Normalized counts ratio between conducive (yellow) and suppressive (black) samples for ASVs from the network in panel B.

Frequently, the germination and growth of plant pathogenic fungi are negatively affected by direct or indirect contact with soils (without the presence of a host plant). This phenomenon is named soil fungistasis (Garbeva et al., 2011; Watson and Ford, 1972) and is often associated with general disease suppressiveness. Whereas abiotic soil factors can be involved, the major cause of fungistasis is biological since it is strongly reduced after soil sterilization, which is analogous to the soil disease suppressiveness. Recent studies revealed that microbial volatiles play important roles in both soil fungistasis as well as disease suppressiveness (Effmert et al., 2012; van Agtmaal et al., 2018). Our study did not reveal any congruence between volatile-mediated soil fungistasis and disease suppressiveness. Volatile-mediated soil suppressiveness was observed only with four soils, including both two suppressive and two conducive soils. This indicates that, even though volatile emission is one of the factors that may contribute to disease suppressiveness to *F. culmorum*, it is not a general one. Apparently, other (complementary) factors and mechanisms are needed to develop a full protective potential against *F. culmorum*. Alternatively, it might be that suppressiveness across the four soils is mediated by different mechanisms, involving volatiles in some cases but not in others. This could also explain the lack of commonly enriched taxa across the four suppressive soils.

In conclusion, we discovered several agricultural soils that protect wheat plants from *Fusarium culmorum* infections through a microbial component. Moreover, these suppressive soils revealed different bacterial taxonomic patterns and diversity, as well as variable degrees of antifungal volatile emissions. These observations reject the hypothesis that specific rhizobacterial taxa and specific volatiles correlate with suppressiveness of *F. culmorum.*

Co-occurrence network analysis suggested that two of the suppressive samples share a similar microbial basis of the phenotype through a uniquely overrepresented bacterial guild dominated by *Acidobacteria*. Of course, taxonomic profiling alone cannot provide definitive answers on the actual biological mechanisms responsible for the suppressive phenotype. Accordingly, we anticipate our work to lay the foundation for a combination of functional metagenomics along with microbiological and biochemical analyses, in order to elucidate the functional mechanisms behind soil suppressiveness to *F. culmorum* in the near future.

Supplementary material

Material and methods

Soil physical and chemical parameters

Soil physical and chemical parameters were measured in triplicate using three independent sub-samples. The soil pH was measured in water and soil organic matter content was determined by loss of ignition, both using standard laboratory methods. Bioavailable iron, potassium, magnesium, phosphorus and sulfur were extracted using 0,01M $CaCl_2$ (VWR, Netherlands) and concentrations were measured with ICP-OES (iCAP 6500 ICP-OES Duo ,Thermo Scientific). Carbon and nitrogen content were determined using an Element Analyser (Flash EA 1112 ,Thermo Scientific).

Disease symptoms assessment

To assess disease symptoms, the wheat plants were carefully removed, the excess of soil was shaken and roots were cleaned in water. The root system was visually inspected for brown/black lesions or rotting, and the stem base/coleoptile was inspected for rotting and the presence of pink-white fungal hyphae. Plants were scored for disease symptoms from 0-5: 0- healthy plants; 1- one or two dark lesions on the roots up to 10 mm; 2- lesions bigger than 10 mm; 3- large lesions on the roots and/or stem base rot; 4- visible pink-white fungal hyphae on the stem with shoot discoloration, extensive root lesions, or stem base rot (at least two of this symptoms); and 5- dead plants (for examples see figure S6). Statistical differences in disease symptoms between treatments and control were assessed using the chi-square test, with an alpha cutoff of $p<0.05$.

Rhizosphere DNA extraction and sequencing

At the end of the experiments, plants were gently removed from the trays. Soil loosely adhering to the roots was removed by shaking. The roots with surrounding soil were placed on a sterile filter in a laminar flow cabinet and the soil particles adhering to the roots were collected using a brush. DNA was immediately isolated using a DNeasy PowerSoil Kit (QIAGEN, the Netherlands) according to manufactures protocol using 0.25 g of rhizosphere soil. Samples were additionally purified using DNeasy PowerClean cleanup kit (QIAGEN, the Netherlands). Sequencing of the bacterial V3-V4 region of the 16S rRNA gene (with primers 16S_V3-341F 5'-CCTACGGGNGGCWGCAG and 16S_V4-785R 5'-GACTACHVGGGTATCTAATCC (Herlemann et al., 2011)) was performed at BaseClear (Leiden, the Netherlands) using Illumina MiSeq in 4 biological replicates per treatment.

Amplicon assembly and taxonomical assignment

The 16S rRNA gene sequencing yielded a total of 4,966,035 reads, sequencing depths for all samples is reported in table S2. Reads were quality-filtered using a sliding window approach of five nucleotides and a Phred score threshold of 30 (Bolger et al., 2014). Forward and reverse reads were then truncated at 280 and 220 bp in length, respectively. The Dada2 (B. J. Callahan et al., 2016) pipeline from Qiime2 (Caporaso et al., 2010) was used to denoise and obtain amplicon sequence variants (ASVs) from demultiplexed reads for all 112 samples. Reads that did not overlap were removed from the rest of the analysis. To remove sequences derived from errors that were not corrected during the DADA2 denoising step, ASVs that had fewer than 20 amplicons mapped across all samples and that appeared in less than 4 different samples were removed from further analysis. This resulted in 4,322 reliable ASVs across the 112 samples, while still retaining over 80% of the sequencing information. Taxonomic assignment was performed in Qiime2 using a Bayesian classifier (Bokulich et al., 2018; Pedregosa et al., 2011) built for the primer pairs used in this study (341F and 805R) on the SILVA release 132 database ref NR 99. The resulting feature count tables were logCSS-normalized in R using the metagenomeSeq library (Paulson et al., 2013). Alpha/beta diversity and clustering of samples using different metrics were calculated with Qiime2 and python skbio library.

Principal coordinate analysis of the amplicon data

Principal coordinate analysis (PCoA) was performed in Qiime2 using Bray-Curtis dissimilarity, Jaccard index, weighted UniFrac and unweighted Unifrac (Lozupone and Knight, 2005). Weighted and unweighted UniFrac distances were calculated in a Python script for all individual bacterial taxonomy groups to reveal existing correlations within taxonomic groups that were being masked by other features. Code for these analyses is available at (https://git.wageningenur.nl/users/traca001/groups).

Identification of suppressive rhizosphere-associated ASVs

ASVs enriched in suppressive and conducive soils were determined with FitZig (Paulson et al., 2013) using the suppressive phenotype as model matrix for hypothesis testing. A strict filter was applied to select ASVs of interest; we consider enriched only ASVs which yielded a p-value below ($p<10^{-10}$) and which occur in at least two different suppressive soil samples (replicates).

Random forest prediction of suppressive soil

Multiple random forest classifiers were built to predict soil phenotype based on its community composition. The classifiers are built with python scikit-learn library bootstrapping the selection of suppressive and conducive samples used to train and test

the model. For each classifier, 3 suppressive and 12 conducive samples are randomly chosen and the remaining samples are used to test the classifier predictions. None of the suppressive sample phenotype could be correctly predicted by the classifier.

Co-occurrence network analysis

Spearman's rank correlation coefficient was calculated using the normalized feature table for all ASV pairs across all samples. Clusters of highly correlated ASVs were obtained by applying a static threshold that preserved only correlations above 0.8, corresponding to approximately 1% of the nonzero interactions. Clusters which contained suppression-associated ASVs as determined by FitZig were further investigated to identify suppression-specific ASV clusters. Network visualization was performed in Cytoscape (Shannon et al., 2003); nodes in the network represent the different ASVs and edges were drawn between pairs of ASVs having a Spearman correlation score above the 0.8 threshold.

Effects of soil-emitted volatiles on fungal growth

To investigate the antifungal activity of the volatiles emitted by eight selected soils on the growth of Fusarium culmorum PV, the bottom-top approach was applied as described previously by Garbeva et al., (Garbeva et al., 2014b) with small modifications. The top part of the experimental system contained a Petri dish with 20 ml of 1/2 PDA medium and a 6 mm Fusarium culmorum PV plug placed in the center, whereas 30 g of soil was added at the bottom. The two parts where separated with a 30 µm sterile nylon mesh (Sefar, Switzerland) to allow exchange of volatile compounds but prevent exchange of spores and soil particles. The whole system was fixed together with paper medical tape (Kruidvat, the Netherlands). The scheme of the system is shown on figure 3A. After seven days at 20°C in the dark, fungal hyphae were harvested, lyophilized and weighed. Every treatment was replicated five times.

Volatile trapping and GC-MS analysis

Volatiles emitted by the eight suppressive and conducive soils were collected in a steel trap with 150 mg Tenax TA and 150 mg Carbopack B (Markes International Ltd, Llantrisant, UK). A perforated steel tube was placed in the glass pot with tested soil mixed with F. culmorum PV agar plugs. The pre-germinated wheat seedling was introduced to this system and after one week of growth, the steel trap was connected to tubes present in the soil for 16h. Every soil was tested in three independent biological replicates. After removing, traps were capped and stored at 4°C until GC-Q-TOF analysis. Volatiles were desorbed from the traps using an automated thermodesorption unit (model UnityTD-100, Markes International Ltd., Llantrisant, UK) at 210°C for 12 min (Helium flow 50 mL/min) and trapped on the cold trap at -10°C. The trapped volatiles were introduced into the GC-QTOF (model Agilent 7890B GC

and the Agilent 7200AB QTOF, Santa Clara, USA) by heating the cold trap for 3 min to 280°C with the split ratio set to 1:10. The column used was a 30 × 0.25 mm DB-5MS UI, film thickness 0.25 µm (122-5532UI, Agilent J&W, USA). Temperature program used was as follows: 39°C for 2 min, from 39°C to 95°C at 3.5°C/min, then to 165°C at 6°C/min, to 250°C at 15°C/min and finally to 300°C at 40°C/min, hold 20 min. The volatiles were detected by the MS operating at 70 eV in EI mode. Mass spectra were acquired in full scan mode (30–400 amu, 4 scans/s). For the volatilomics analysis, the acquired raw mass spectrometry (MS) data was extracted to m/z format using MassHunter Qualitative Analysis Software V B.07.00 (Agilent Technologies, Santa Clara, CA, USA). The m/z data was processed with MZMine V 2.36 (Copyright © 2005–2012 MZmine Development Team, (Pluskal et al., 2010)) as described in (Lankenau et al., 2015) to create an m/z and peak intensity table that could be used as input file for MetaboAnalyst 4.0 software (http://www.metaboanalyst.ca/MetaboAnalyst (Chong et al., 2018)). Before the statistical analysis, the data was filtered using Interquantile range (IQR) and normalized by the log transformation with automatic scaling.

Table S1. Table presenting physical and chemical characteristics of the soils and the crops grown in the fields in 3 seasons before the collection

soil	pH	SD	OM	SD	Fe	SD	K	SD	Mg	SD	P	SD	S	SD	C	SD	N	SD	C:N	soil type	2016	2015	2014
BS	7.53	0.05	0.24	0.04	0.19	0.01	2.02	0.32	0.00	0.00	0.11	0.03	0.00	0.00	0.05	0.01	0.00	0.00	NA	Sand	-	-	-
S01	6.22	0.17	3.46	0.35	0.09	0.00	34.00	0.92	163.19	1.75	1.40	0.01	1.29	0.08	2.31	0.18	0.14	0.01	16.50	Sand	-	-	-
S02	6.75	0.04	3.81	0.08	0.03	0.00	86.66	2.38	36.86	0.79	0.89	0.02	2.50	0.15	1.60	0.08	0.11	0.01	14.55	Clay	Wheat	Potatoes	Wheat
S03	5.28	0.27	5.49	0.68	0.45	0.06	59.95	2.29	56.74	2.11	2.69	0.08	2.60	0.16	3.77	1.13	0.26	0.10	14.50	Sand	Winter wheat	Winter wheat	Winter wheat
S04	7.30	0.30	3.10	0.29	0.02	0.00	117.12	1.20	56.49	0.25	1.53	0.05	7.21	0.99	2.11	0.02	0.13	0.00	16.23	Clay	Wheat	Onions	Lucerne
S05	6.47	0.10	3.56	0.37	0.16	0.00	109.72	2.16	74.87	1.58	7.76	0.32	1.29	0.18	1.99	0.53	0.16	0.04	12.44	Clay	Winter wheat	Potatoes	Winter wheat
S06	7.58	0.02	3.51	0.40	0.05	0.00	223.26	1.92	84.60	0.92	2.62	0.08	12.23	0.85	2.72	1.11	0.19	0.10	14.32	Sandy loam	Rye	Leaf vegetables	Winter wheat
S07	7.58	0.06	4.32	0.36	0.03	0.00	82.92	1.74	61.11	0.43	1.66	0.05	5.57	0.07	2.92	0.11	0.18	0.01	16.22	Sand	Winter wheat	Potatoes	Winter wheat
S08	6.87	0.06	2.81	0.51	0.08	0.00	181.54	3.76	109.68	1.70	16.23	0.05	1.14	0.05	1.94	0.24	0.16	0.01	12.13	Sand	Spring wheat	Pattison/ yakon	Pattison/ yakon
S09	6.87	0.18	3.26	0.32	0.06	0.01	174.31	1.13	113.01	0.78	3.06	0.07	1.26	0.22	1.35	0.14	0.12	0.01	11.25	Sand	Spring wheat	Onions	Sweet corn
S10	7.49	0.04	2.92	0.44	0.02	0.00	97.07	2.67	70.88	0.54	1.12	0.07	2.96	0.05	2.62	0.13	0.16	0.01	16.38	Clay	Spelt	Peas	Beetroot/pumpkins
S11	7.28	0.19	3.48	0.47	0.11	0.00	68.77	1.10	56.43	0.58	5.43	0.04	1.17	0.15	1.99	0.88	0.16	0.07	12.44	Sand	Luzerne/grass	Luzerne/grass	Barley
S12	7.75	0.01	3.81	0.32	0.02	0.00	233.38	0.68	83.72	0.95	1.06	0.01	9.00	0.29	2.03	0.35	0.14	0.04	14.50	Clay	Celery	Cabbage	Grass clover
S13	7.55	0.14	7.03	0.25	0.04	0.00	207.13	4.04	122.52	1.44	3.40	0.12	7.57	0.06	3.82	0.01	0.34	0.00	11.24	Clay	Grass clover	Grass clover	Red cabbage
S14	7.61	0.05	5.04	0.35	0.04	0.00	82.49	4.08	98.91	4.04	0.70	0.06	8.61	0.08	2.35	0.14	0.15	0.01	15.67	Sandy clay	Winter wheat	Beetroot	Potatoes
S15	7.82	0.05	3.77	0.63	0.02	0.00	45.83	0.53	60.60	0.52	0.90	0.05	5.95	0.06	1.91	0.08	0.11	0.01	17.36	Clay	Potatoes	Grass clover	Onions
S16	7.63	0.12	2.91	0.57	0.03	0.00	53.60	0.85	78.47	0.42	5.61	0.17	2.79	0.21	2.33	1.44	0.18	0.13	12.94	Clay	Luzerne	Potatoes	Carrots
S17	7.75	0.06	4.23	0.79	0.01	0.00	87.17	2.45	74.54	0.80	1.03	0.04	2.27	0.06	2.63	0.05	0.15	0.00	17.53	Clay	Potatoes	Spelt	Pumpkins
S18	7.69	0.06	7.53	0.94	0.02	0.00	53.59	0.56	113.54	0.51	1.49	0.06	5.80	0.37	2.30	0.02	0.24	0.00	9.58	Clay	Winter wheat	Winter wheat	Winter wheat
S19	7.73	0.02	5.38	0.50	0.02	0.01	63.09	0.68	104.28	2.48	1.50	0.01	5.00	0.28	2.35	0.02	0.24	0.00	9.79	Clay	Winter wheat	Winter wheat	Sugar beet
S20	7.30	0.16	8.00	0.21	0.10	0.00	234.45	3.76	299.63	6.42	2.69	0.02	6.98	0.41	3.25	0.65	0.36	0.10	9.03	Sand	Maize	Maize	Winter wheat
S21	5.56	0.12	20.59	1.00	0.82	0.07	58.82	4.26	484.44	14.16	4.86	0.10	24.70	0.13	9.30	0.39	1.04	0.03	8.94	Sand	Pasture	Pasture	Pasture
S22	6.50	0.10	3.02	0.48	0.03	0.01	74.84	1.84	237.38	3.52	0.87	0.09	3.67	0.15	2.65	0.10	0.30	0.01	8.83	Clay	Maize	Winter wheat	Sugar beet
S23	5.92	0.39	4.50	0.50	0.47	0.04	51.98	1.52	122.23	3.32	11.88	0.27	4.03	0.29	1.92	0.60	0.17	0.05	11.29	Sand	Grass clover	Maize	Maize
S24	7.27	0.06	6.15	0.38	0.02	0.00	76.47	1.19	66.70	0.61	2.58	0.12	5.24	0.45	0.98	0.07	0.11	0.00	8.91	Clay	Wheat	Beetroot	Wheat
S25	5.35	0.15	7.34	0.55	0.24	0.04	57.68	12.82	83.30	3.25	1.26	0.05	5.61	1.70	3.17	0.03	0.26	0.01	12.19	Clay	Forest	Forest	Forest
S26	5.76	0.05	8.54	1.92	0.12	0.01	27.52	2.83	113.43	0.69	1.41	0.14	3.50	0.46	3.13	0.12	0.32	0.01	9.78	Clay	Pasture	Pasture	Pasture
S27	7.05	0.04	7.86	0.94	0.04	0.01	52.66	2.86	98.95	2.37	0.85	0.04	4.53	0.47	3.21	0.14	0.31	0.01	10.35	Clay	Winter rape	Winter wheat	Winter rape
S28	7.13	0.07	3.29	0.12	0.02	0.00	71.36	0.44	160.26	2.70	0.79	0.02	1.74	0.24	1.52	0.01	0.17	0.00	8.94	Clay	Winter wheat	Winter wheat	Winter rape

* to highlight the differences in the measured parameters, pH values are colored from red to blue, showing low to high values respectively.
Other parameters: organic matter content (OM), content of bioavailable elements (Fe, K, Mg, P, S), total carbon (C) and nitrogen (N) are colored with green bars according to their normalized values. Presented values are average of three replicates with standard deviations (SD).
Column “soil”: soil samples in the collection S01 to S28 and BS: “Bergharen soil” used as a standard substrate in the study.

Table S2. Sequencing depths for all rhizosphere samples, the value following underscore indicates the replicate number.

sample-id	input	filtered	denoised	merged	non-chimeric
S01_1	41725	33607	33607	17264	16866
S01_2	45462	36178	36178	19858	19373
S01_3	41822	33415	33415	17196	16778
S01_4	49352	39531	39531	25025	23379
S02_1	53186	42592	42592	23199	22708
S02_2	42743	33988	33988	17520	17061
S02_3	54037	42031	42031	24111	23450
S02_4	43360	34930	34930	19538	19008
S03_1	44954	36506	36506	20855	19746
S03_2	42219	33757	33757	19801	18422
S03_3	46183	36515	36515	18537	17677
S03_4	46941	38080	38080	26964	21045
S04_1	49195	39946	39946	22155	21807
S04_2	49236	39690	39690	21736	21295
S04_3	47442	38178	38178	18923	18293
S04_4	49544	39379	39379	21418	21023
S05_1	49240	39988	39988	22254	21030
S05_2	48264	39067	39067	22833	19870
S05_3	49934	39348	39348	21713	20461
S05_4	39082	31770	31770	15274	14745
S06_1	36164	28958	28958	14296	13856
S06_2	42717	33193	33193	17723	17161
S06_3	45214	36400	36400	19923	19316
S06_4	48268	39142	39142	22538	21914
S07_1	53097	43001	43001	24869	23953
S07_2	45927	36549	36549	20537	19901
S07_3	63205	50499	50499	28516	27743
S07_4	33926	23095	23095	11884	11526
S08_1	46293	36945	36945	19611	18169
S08_2	44794	35469	35469	17577	17171
S08_3	49441	39931	39931	20719	20031
S08_4	37841	30283	30283	15807	15425
S09_1	50458	40629	40629	20554	19966

S09_2	49480	40250	40250	21995	20986
S09_3	52163	41629	41629	21864	21281
S09_4	42913	34941	34941	20271	19325
S10_1	46209	37005	37005	19507	18922
S10_2	50250	40050	40050	22734	21712
S10_3	48066	38386	38386	20345	19824
S10_4	49532	39101	39101	21937	21262
S11_1	56437	45456	45456	23637	22725
S11_2	39385	31551	31551	17438	16721
S11_3	53460	42318	42318	25257	21916
S11_4	50498	40678	40678	23542	22765
S12_1	45994	36824	36824	20278	19617
S12_2	51667	41515	41515	21963	21437
S12_3	45604	36075	36075	18933	18300
S12_4	51902	41044	41044	21966	21488
S13_1	51177	36785	36785	19145	18648
S13_2	41781	24407	24407	11186	10807
S13_3	49981	35778	35778	18301	17694
S13_4	52143	36067	36067	19093	18040
S14_1	43642	34264	34264	16925	16489
S14_2	48616	35195	35195	17718	17067
S14_3	44910	35575	35575	19273	18733
S14_4	46545	37762	37762	19310	18766
S15_1	42858	34576	34576	21410	19796
S15_2	44762	36195	36195	21763	20477
S15_3	47422	37758	37758	22556	20948
S15_4	40163	32478	32478	19295	17778
S16_1	37249	29402	29402	17735	15462
S16_2	42173	33561	33561	19422	17928
S16_3	45586	35797	35797	19070	18582
S16_4	47442	37272	37272	20494	19546
S17_1	51215	40873	40873	23147	22687
S17_2	36361	28296	28296	15250	14910
S17_3	46849	35967	35967	21923	20765
S17_4	34766	27361	27361	15537	14981
S18_1	41336	32946	32946	20058	19553

S18_2	40194	32632	32632	22587	20284
S18_3	42221	33277	33277	20019	19251
S18_4	46846	37084	37084	22159	21539
S19_1	46160	37438	37438	20790	19621
S19_2	50469	40792	40792	25392	24178
S19_3	48494	38879	38879	22395	21824
S19_4	47951	38527	38527	21996	21417
S20_1	47183	38076	38076	21987	20928
S20_2	42260	34401	34401	18843	17951
S20_3	50901	40503	40503	24416	23098
S20_4	46791	37990	37990	21608	20737
S21_1	41015	33565	33565	20978	19475
S21_2	42477	34136	34136	22696	20685
S21_3	40303	32376	32376	20665	18926
S21_4	48019	38702	38702	25304	23038
S22_1	40909	32639	32639	18592	17702
S22_2	41907	33008	33008	19844	19022
S22_3	39314	30697	30697	16937	16152
S22_4	38281	29928	29928	16296	15277
S23_1	40319	31358	31358	18190	17451
S23_2	37341	29756	29756	16975	16319
S23_3	44530	34840	34840	24350	23209
S23_4	32947	26534	26534	17998	15700
S24_1	33962	27307	27307	18314	16753
S24_2	28800	21596	21596	12698	12206
S24_3	37292	29303	29303	17886	17219
S24_4	34107	27271	27271	15776	15092
S25_1	49186	38629	38629	23479	22078
S25_2	34056	27924	27924	17522	16205
S25_3	33382	26871	26871	16546	15777
S25_4	46462	37279	37279	23340	22028
S26_1	44438	35281	35281	24243	22827
S26_2	35931	28941	28941	18414	17321
S26_3	41725	33546	33546	21393	20124
S26_4	38662	30842	30842	19765	18296
S27_1	43453	34538	34538	18675	17996

S27_2	36183	29045	29045	16110	15616
S27_3	35734	29053	29053	17498	16072
S27_4	45394	36708	36708	20020	19196
S28_1	36616	29403	29403	17577	16093
S28_2	31889	26103	26103	15858	14455
S28_3	34760	27914	27914	16259	15566
S28_4	45368	36476	36476	21778	20336

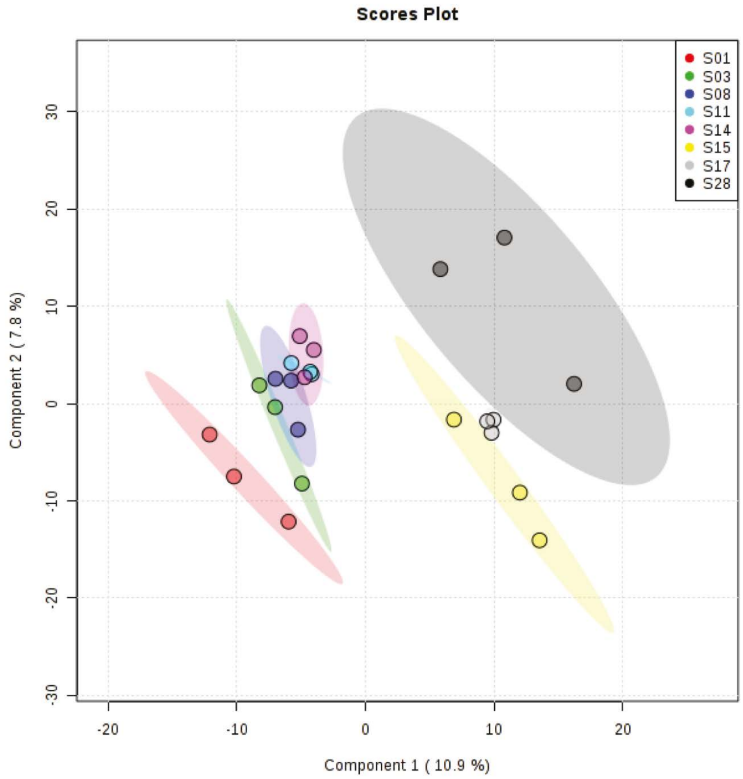

Figure S3. PCoA plot showing GC-MS profiles of volatile compounds emitted by eight soils, four suppressive (S01, S03, S11 and S28) and four conducive (S08, S14, S15 and S17) soils.

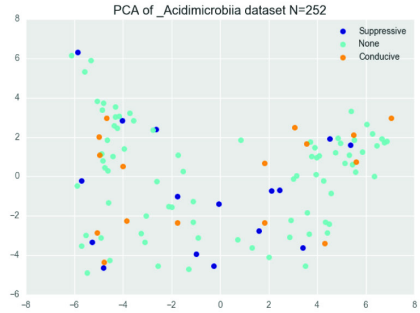
PCA of _Acidimicrobiia dataset N=252
Suppressive
None
Conducive

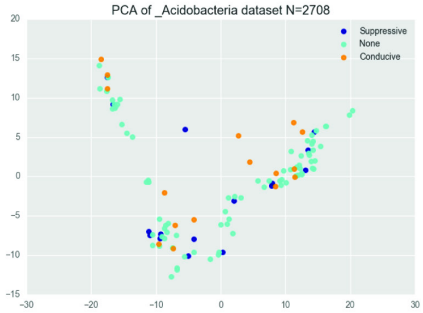
PCA of _Acidobacteria dataset N=2708
Suppressive
None
Conducive

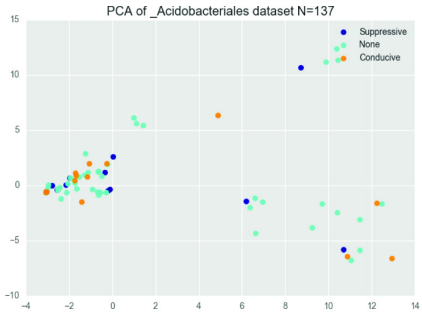
PCA of _Acidobacteriales dataset N=137
Suppressive
None
Conducive

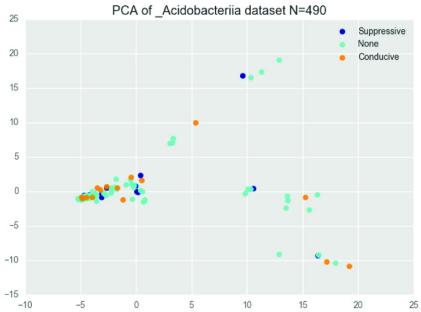
PCA of _Acidobacteriia dataset N=490
Suppressive
None
Conducive

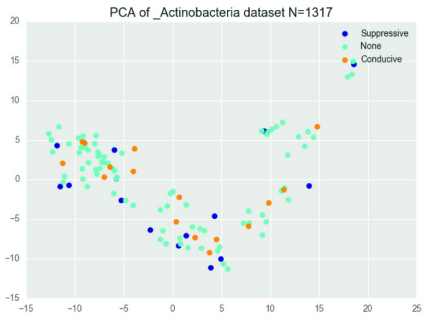
PCA of _Actinobacteria dataset N=1317
Suppressive
None
Conducive

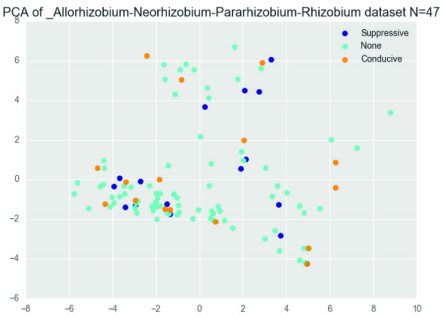
PCA of _Allorhizobium-Neorhizobium-Pararhizobium-Rhizobium dataset N=47
Suppressive
None
Conducive

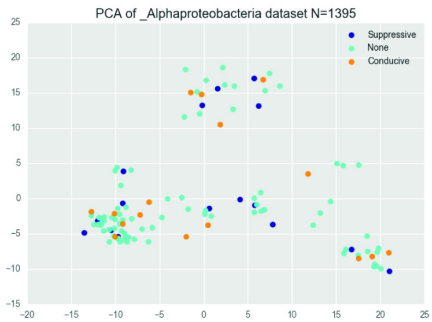
PCA of _Alphaproteobacteria dataset N=1395
Suppressive
None
Conducive

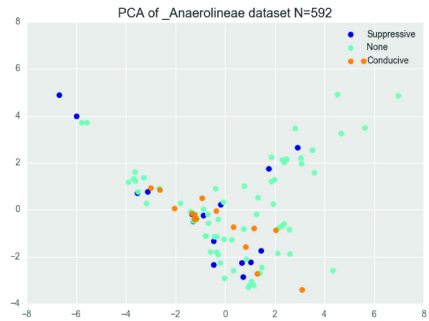
PCA of _Anaerolineae dataset N=592
Suppressive
None
Conducive

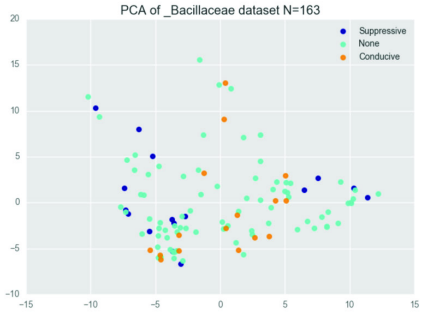
PCA of _Bacillaceae dataset N=163
Suppressive
None
Conducive

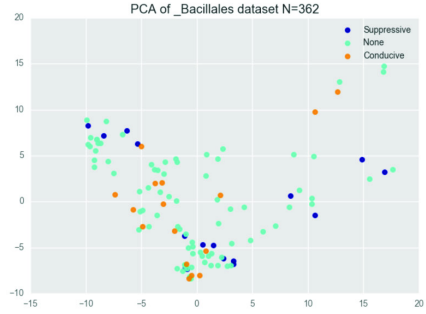
PCA of _Bacillales dataset N=362
Suppressive
None
Conducive

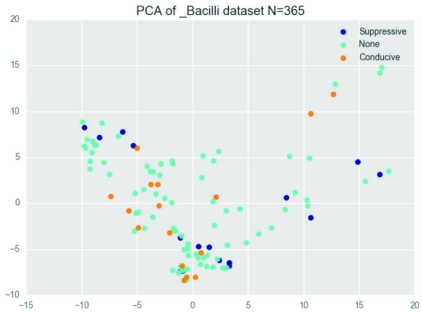
PCA of _Bacilli dataset N=365
Suppressive
None
Conducive

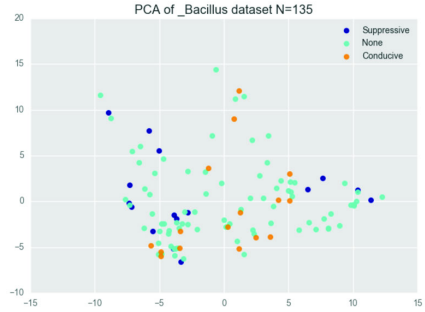
PCA of _Bacillus dataset N=135
Suppressive
None
Conducive

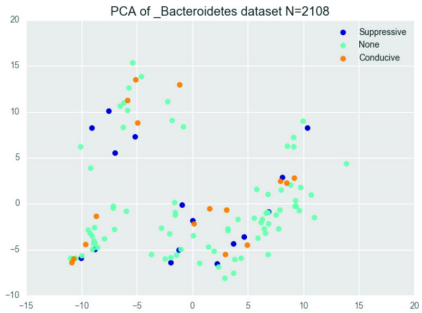
PCA of _Bacteroidetes dataset N=2108
Suppressive
None
Conducive

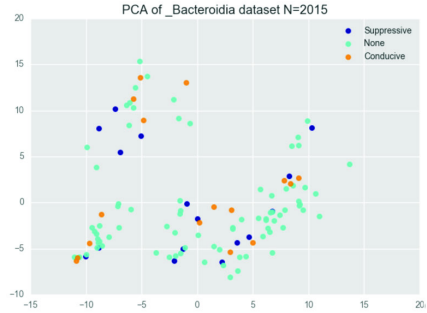
PCA of _Bacteroidia dataset N=2015
Suppressive
None
Conducive

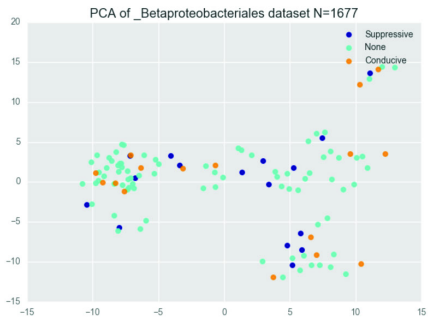
PCA of _Betaproteobacteriales dataset N=1677
Suppressive
None
Conducive

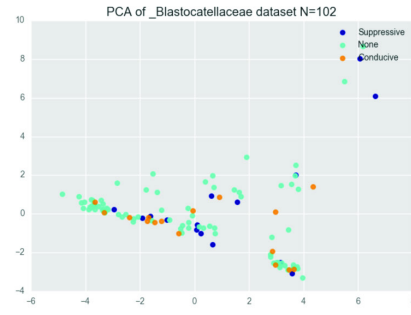
PCA of _Blastocatellaceae dataset N=102
Suppressive
None
Conducive

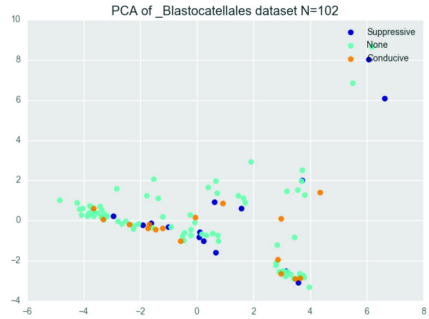
PCA of _Blastocatellales dataset N=102
Suppressive
None
Conducive

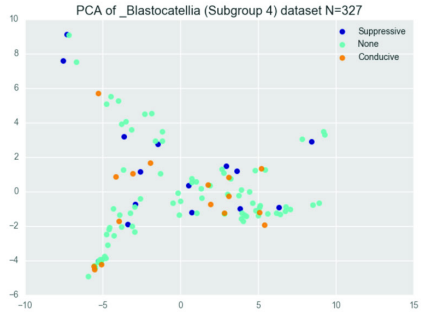
PCA of _Blastocatellia (Subgroup 4) dataset N=327
Suppressive
None
Conducive

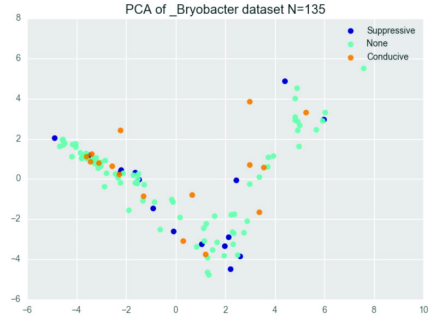
PCA of _Bryobacter dataset N=135
Suppressive
None
Conducive

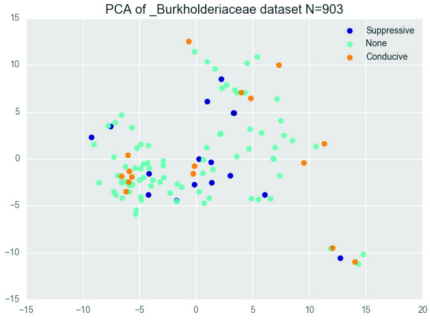
PCA of _Burkholderiaceae dataset N=903
Suppressive
None
Conducive

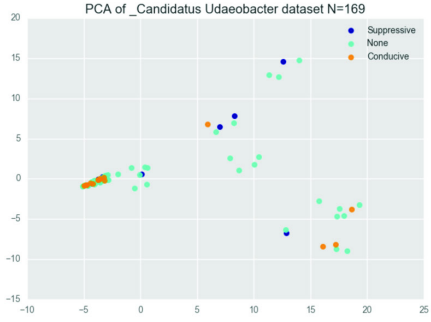
PCA of _Candidatus Udaeobacter dataset N=169
Suppressive
None
Conducive

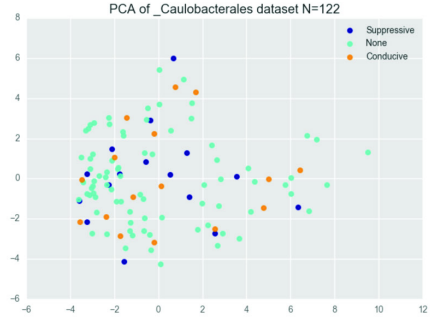
PCA of _Caulobacterales dataset N=122
Suppressive
None
Conducive

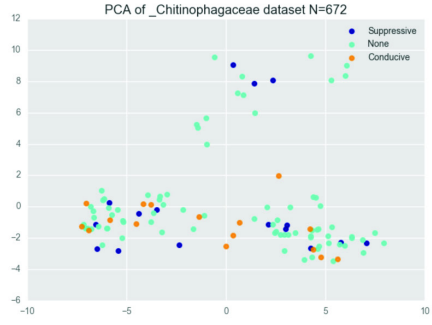
PCA of _Chitinophagaceae dataset N=672
Suppressive
None
Conducive

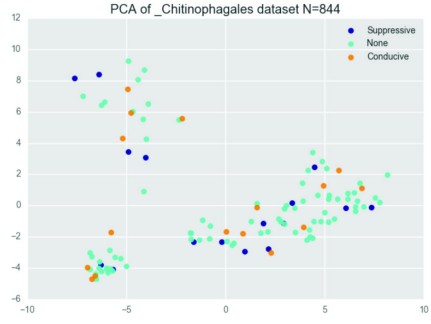
PCA of _Chitinophagales dataset N=844
Suppressive
None
Conducive

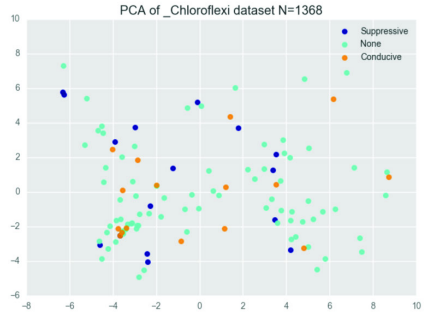
PCA of _Chloroflexi dataset N=1368
Suppressive
None
Conducive

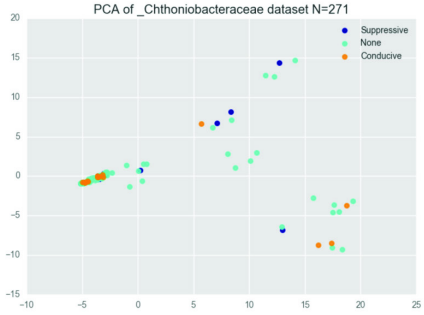
PCA of _Chthoniobacteraceae dataset N=271
Suppressive
None
Conducive

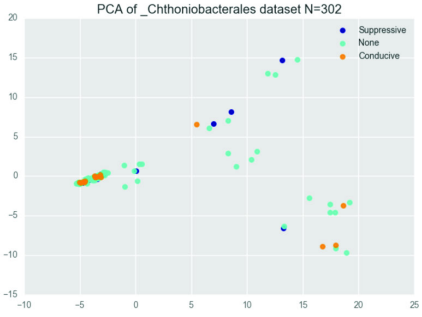
PCA of _Chthoniobacterales dataset N=302
Suppressive
None
Conducive

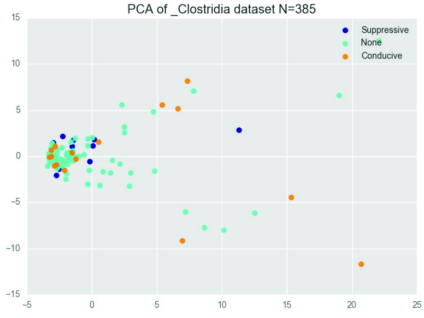
PCA of _Clostridia dataset N=385
Suppressive
None
Conducive

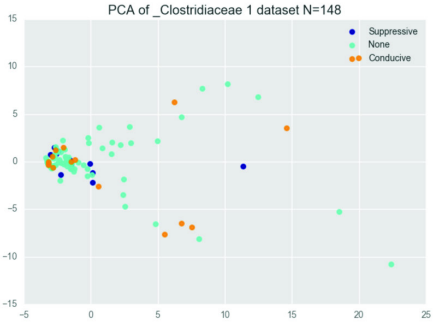
PCA of _Clostridiaceae 1 dataset N=148
Suppressive
None
Conducive

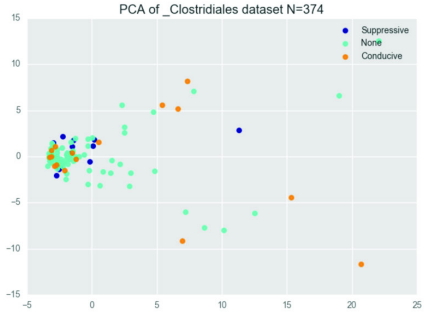
PCA of _Clostridiales dataset N=374
Suppressive
None
Conducive

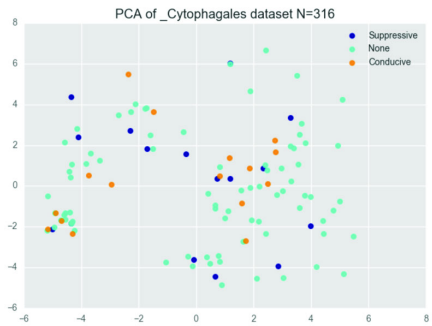
PCA of _Cytophagales dataset N=316
Suppressive
None
Conducive

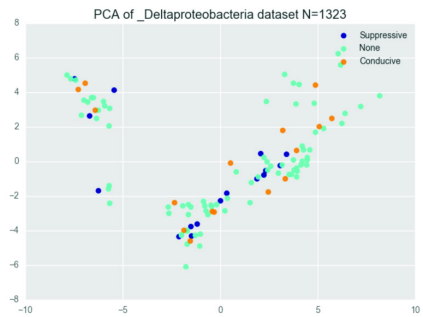
PCA of _Deltaproteobacteria dataset N=1323
Suppressive
None
Conducive

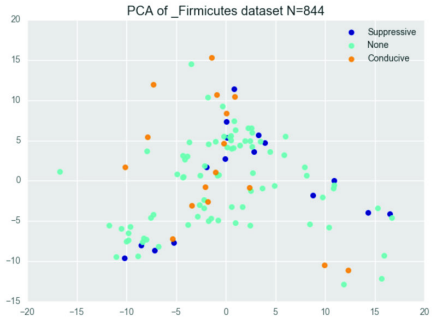
PCA of _Firmicutes dataset N=844
Suppressive
None
Conducive

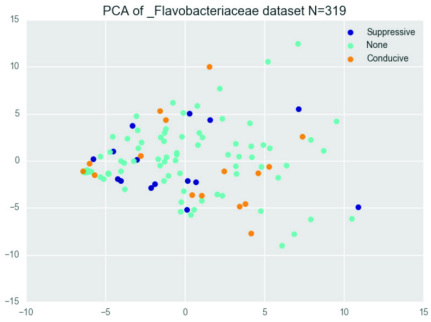
PCA of _Flavobacteriaceae dataset N=319
Suppressive
None
Conducive

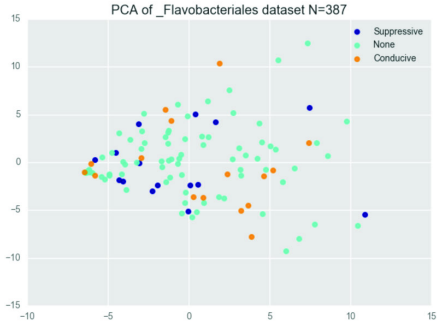
PCA of _Flavobacteriales dataset N=387
Suppressive
None
Conducive

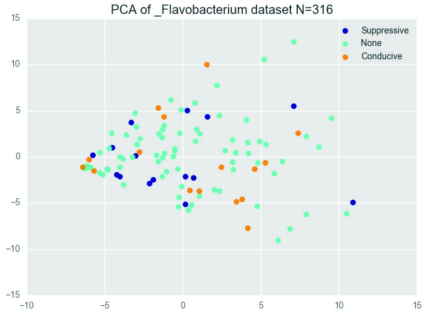
PCA of _Flavobacterium dataset N=316
Suppressive
None
Conducive

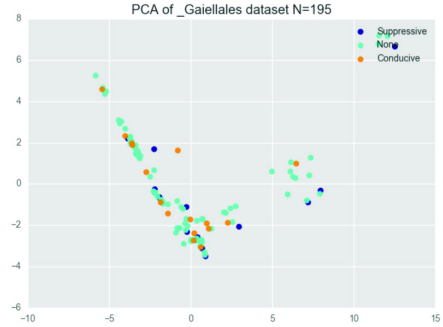
PCA of _Gaiellales dataset N=195
Suppressive
None
Conducive

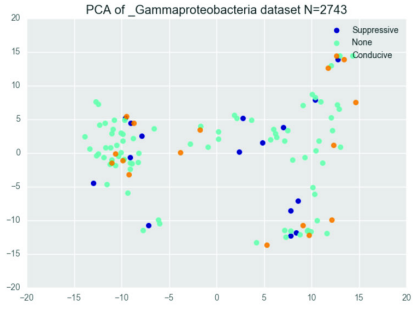
PCA of _Gammaproteobacteria dataset N=2743
Suppressive
None
Conducive

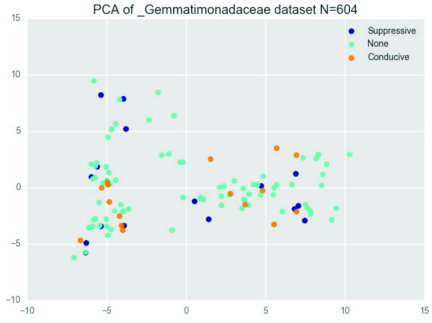
PCA of _Gemmatimonadaceae dataset N=604
Suppressive
None
Conducive

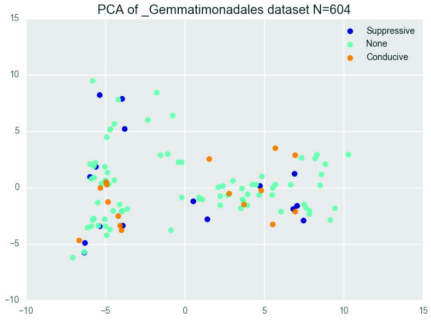
PCA of _Gemmatimonadales dataset N=604
Suppressive
None
Conducive

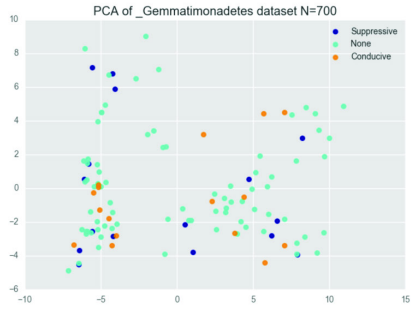
PCA of _Gemmatimonadetes dataset N=700
Suppressive
None
Conducive

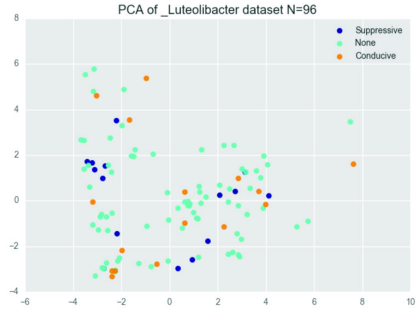
PCA of _Luteolibacter dataset N=96
Suppressive
None
Conducive

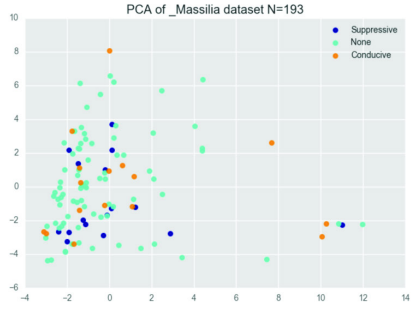
PCA of _Massilia dataset N=193
Suppressive
None
Conducive

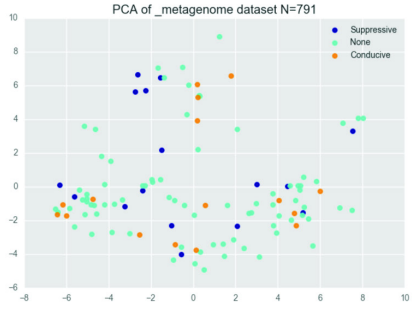
PCA of _metagenome dataset N=791
Suppressive
None
Conducive

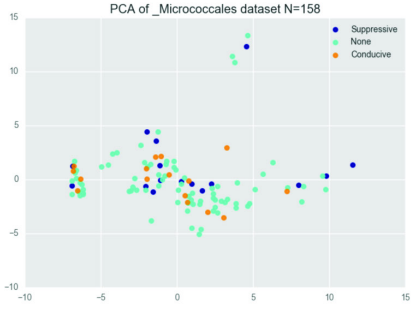
PCA of _Micrococcales dataset N=158
Suppressive
None
Conducive

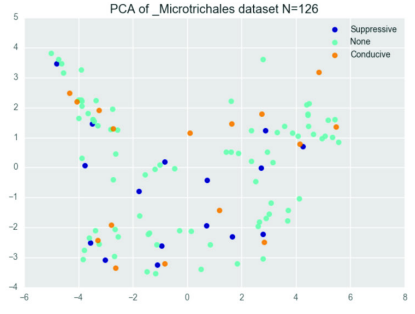
PCA of _Microtrichales dataset N=126
Suppressive
None
Conducive

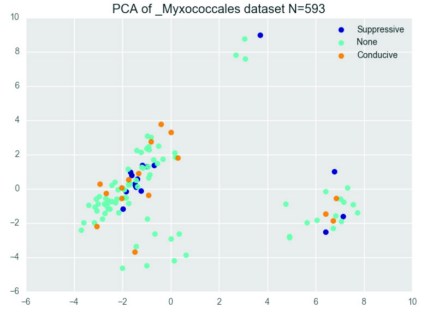
PCA of _Myxococcales dataset N=593
Suppressive
None
Conducive

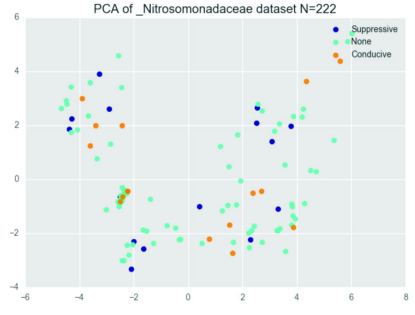
PCA of _Nitrosomonadaceae dataset N=222
Suppressive
None
Conducive

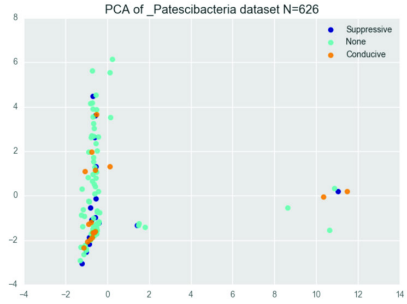
PCA of _Patescibacteria dataset N=626
Suppressive
None
Conducive

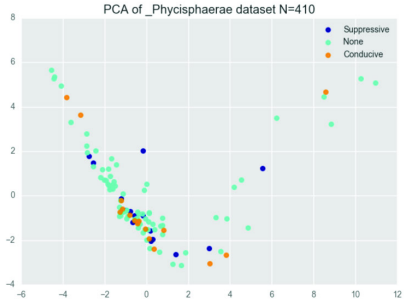
PCA of _Phycisphaerae dataset N=410
Suppressive
None
Conducive

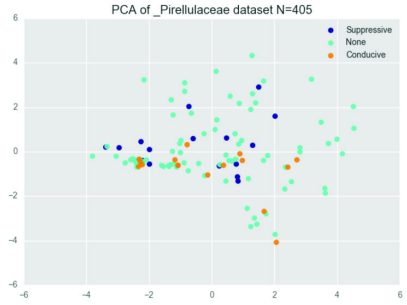
PCA of _Pirellulaceae dataset N=405
Suppressive
None
Conducive

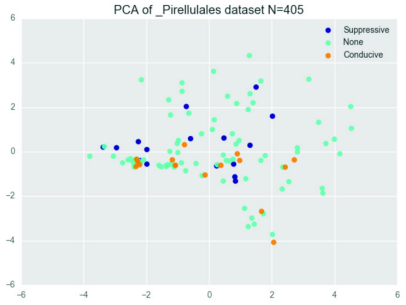
PCA of _Pirellulales dataset N=405
Suppressive
None
Conducive

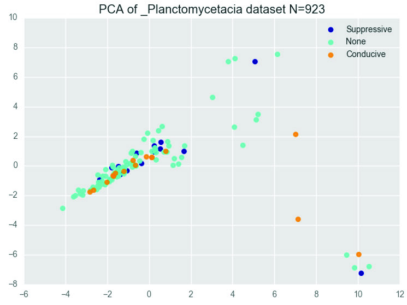
PCA of _Planctomycetacia dataset N=923
Suppressive
None
Conducive

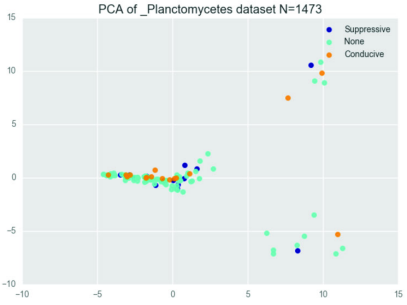
PCA of _Planctomycetes dataset N=1473
Suppressive
None
Conducive

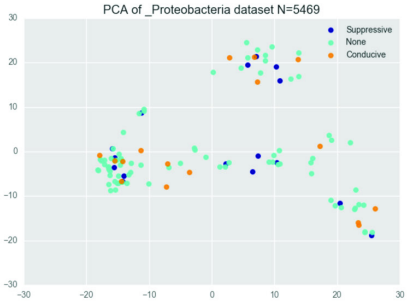
PCA of _Proteobacteria dataset N=5469
Suppressive
None
Conducive

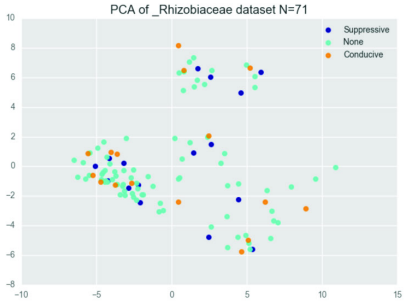
PCA of _Rhizobiaceae dataset N=71
Suppressive
None
Conducive

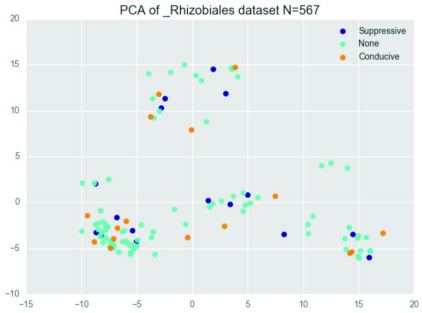
PCA of _Rhizobiales dataset N=567
Suppressive
None
Conducive

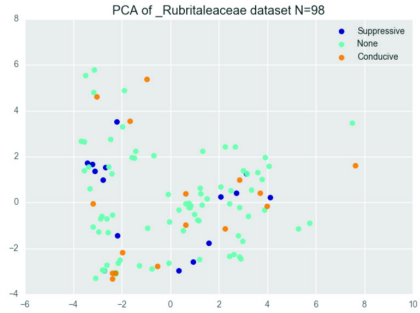
PCA of _Rubritaleaceae dataset N=98
Suppressive
None
Conducive


PCA of _SC-I-84 dataset N=238
Suppressive
None
Conducive

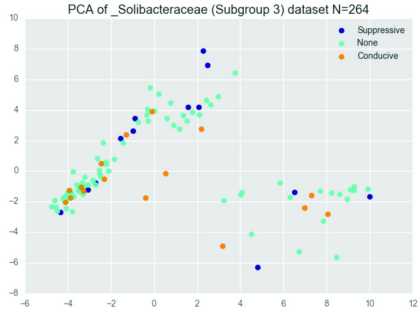
PCA of _Solibacteraceae (Subgroup 3) dataset N=264
Suppressive
None
Conducive

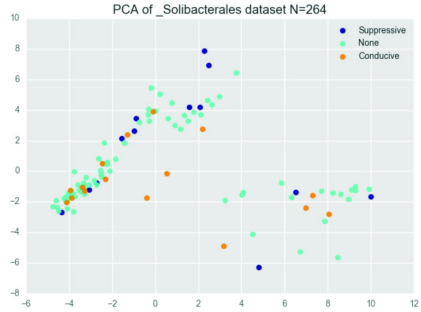
PCA of _Solibacterales dataset N=264
Suppressive
None
Conducive

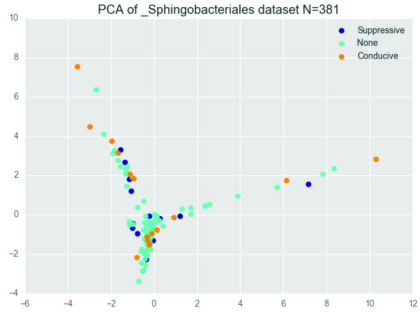
PCA of _Sphingobacteriales dataset N=381
Suppressive
None
Conducive

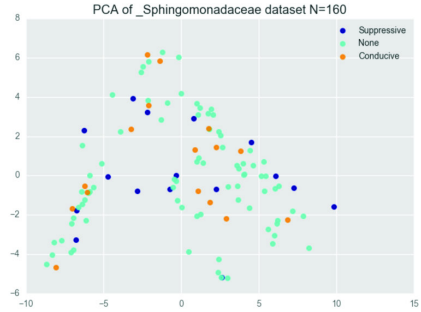
PCA of _Sphingomonadaceae dataset N=160
Suppressive
None
Conducive

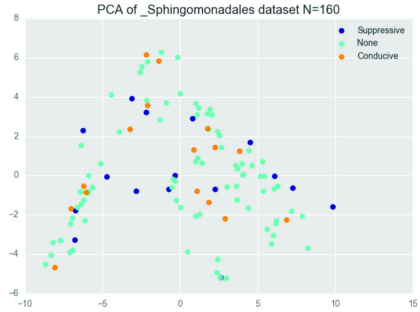
PCA of _Sphingomonadales dataset N=160
Suppressive
None
Conducive

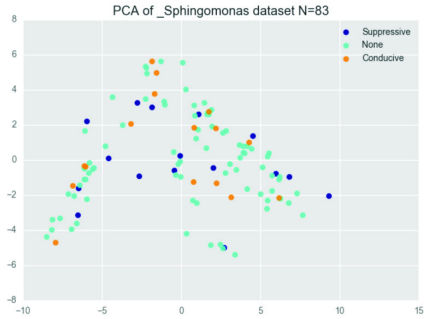
PCA of _Sphingomonas dataset N=83
Suppressive
None
Conducive

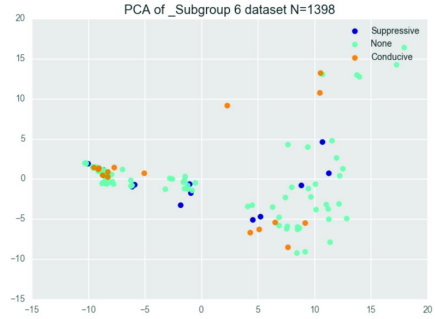
PCA of _Subgroup 6 dataset N=1398
Suppressive
None
Conducive

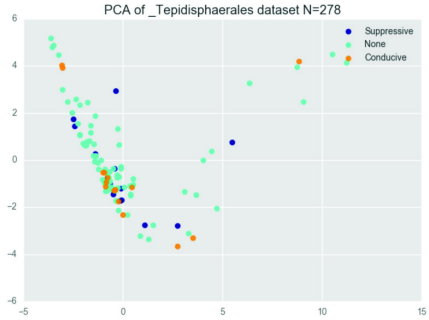
PCA of _Tepidisphaerales dataset N=278
Suppressive
None
Conducive

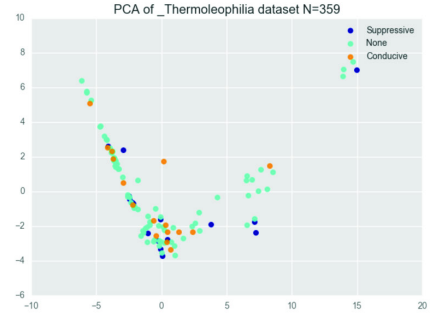
PCA of _Thermoleophilia dataset N=359
Suppressive
None
Conducive

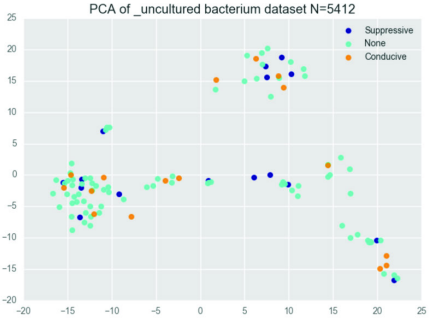
PCA of _uncultured bacterium dataset N=5412
Suppressive
None
Conducive

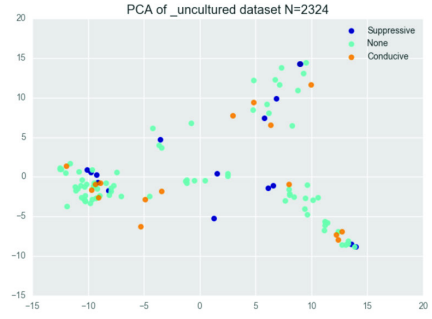
PCA of _uncultured dataset N=2324
Suppressive
None
Conducive

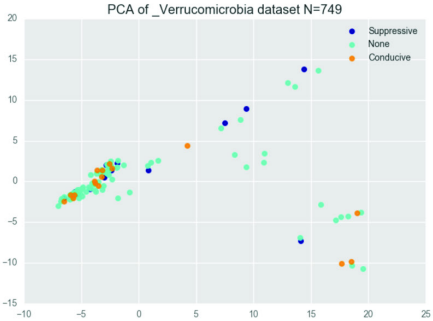
PCA of _Verrucomicrobia dataset N=749
Suppressive
None
Conducive

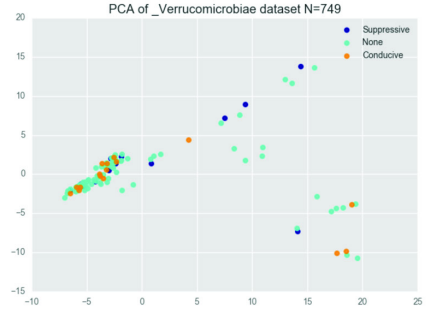
PCA of _Verrucomicrobiae dataset N=749
Suppressive
None
Conducive

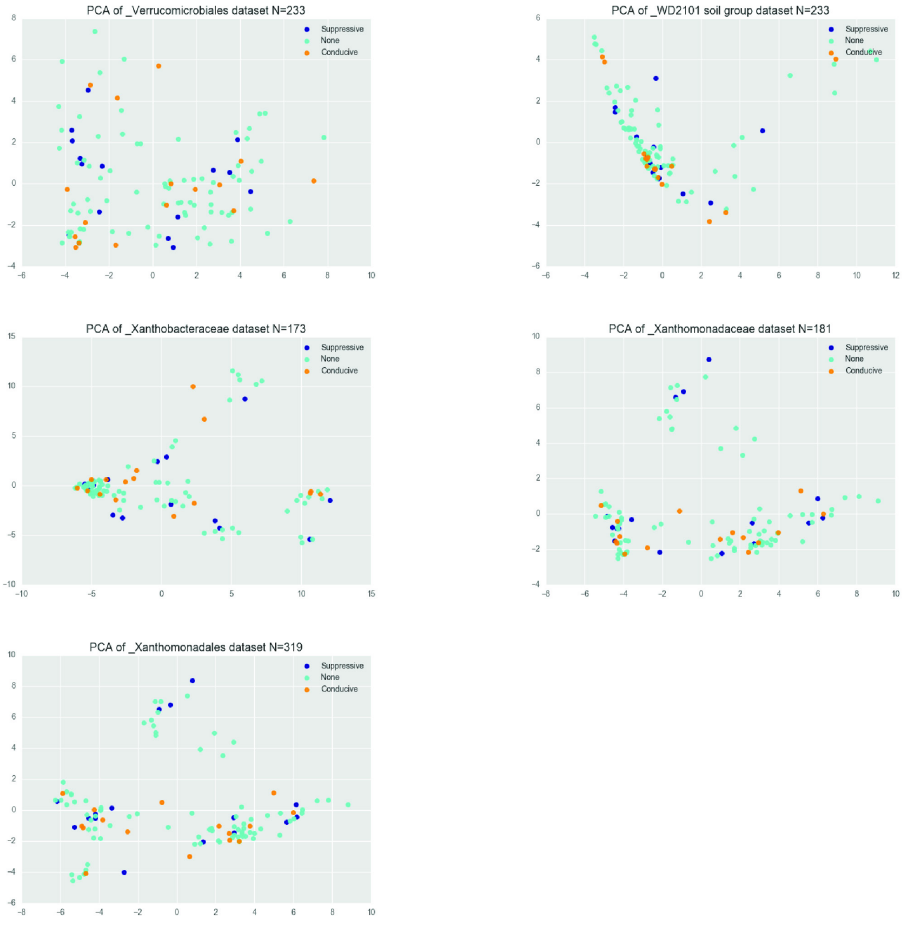

Figure S4. PCA plots of different taxonomy groups. The number of ASVs used for the component analysis is reported on top of each plot together with the taxonomic group represented in the figure.

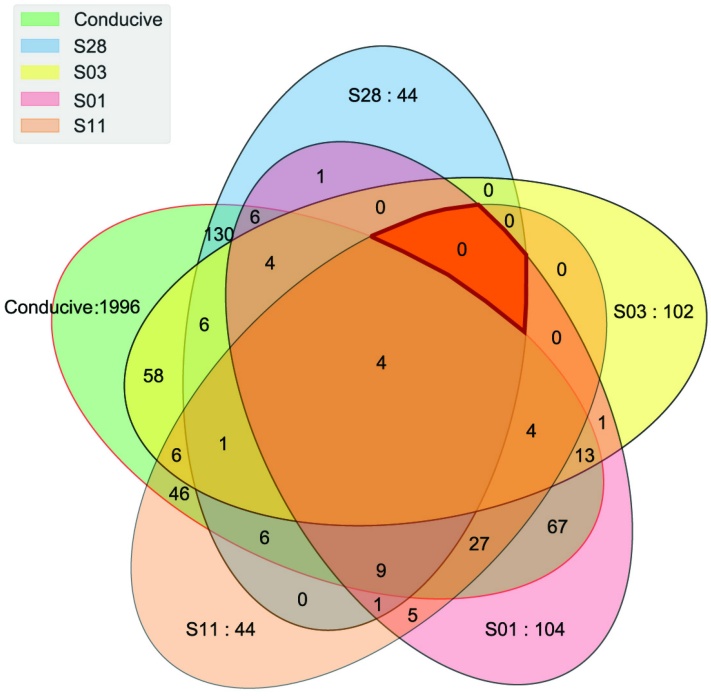

Figure S5. Presence-absence patterns of consistent ASVs. Venn diagram representing the ASVs which consistently appear in all replicates for each of the suppressive samples (S01, S03, S11 and S28) and the conducive samples (here grouped under "conducive").

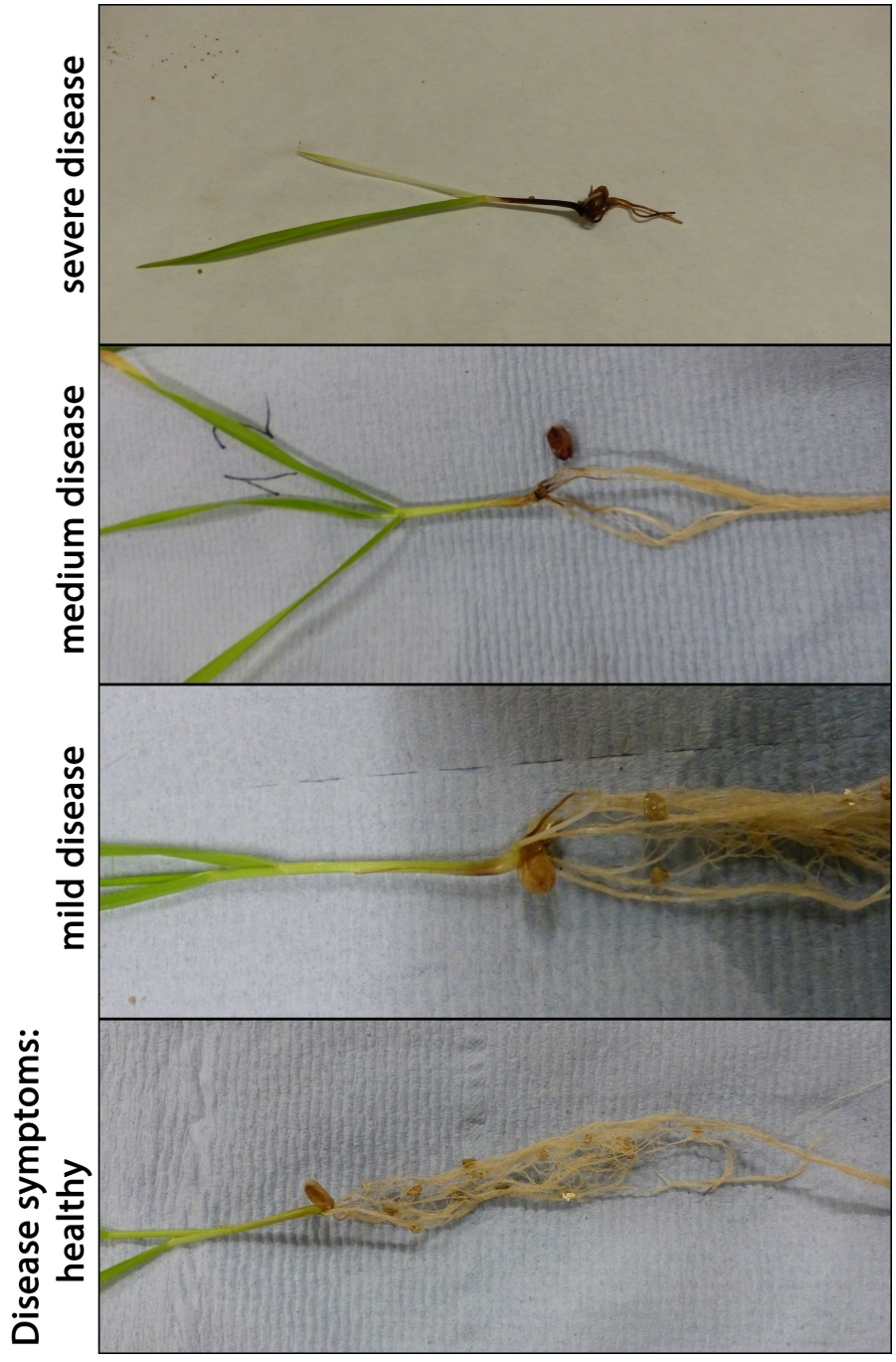

Figure S6. Examples of healthy and diseased plants obtained in the screening with disease scores indicated in brackets.